

The Dial-a-Ride Problem with Limited Pickups per Trip

Boshuai Zhao¹, Kai Wang², Wenchao Wei³, Roel Leus^{1*}

¹KU Leuven, Research Center for Operations Research & Statistics, Belgium

²School of Vehicle and Mobility, Tsinghua University, China

³School of Economics and Management, Beijing Jiaotong University, China

Abstract: The Dial-a-Ride Problem (DARP) is an optimization problem that involves determining optimal routes and schedules for several vehicles to pick up and deliver items at minimum cost. Motivated by real-world carpooling and crowdshipping scenarios, we introduce an additional constraint imposing a maximum number on the number of pickups per trip. This results in the Dial-a-Ride Problem with Limited Pickups per Trip (DARP-LPT). We apply a fragment-based method for DARP-LPT, where a fragment is a partial path. Specifically, we extend two formulations from Rist & Forbes (2021): the Fragment Flow Formulation (FFF) and the Fragment Assignment Formulation (FAF). We establish FFF's superiority over FAF, both from a theoretical as well as from a computational perspective. Furthermore, our results show that FFF and FAF significantly outperform traditional arc-based formulations in terms of solution quality and time. Additionally, compared to the two existing fragment sets, one with longer partial paths and another with shorter ones, our newly generated fragment sets perform better in terms of solution quality and time when fed into FFF.

Keywords: routing, dial-a-ride problem, limited number of pickups per trip, fragments

1 Background

The Dial-a-Ride Problem (DARP) is an optimization problem that involves finding optimal routes and schedules for a fleet of vehicles to pick up and deliver a set of items (passengers or parcels). Each item has a specific pickup and delivery location and time window, and the objective is to schedule the vehicles in a way that minimizes the total travel time or distance, while satisfying various operational constraints such as vehicle capacity, time windows, and pickup and delivery locations.

*Corresponding author: Roel Leus (roel.leus@kuleuven.be)

DARP has found extensive applications in the sharing mobility (Mourad et al., 2019; Tafreshian et al., 2020) and food delivery sectors. Within the sharing mobility domain, the ride-sharing routing problem represents a variant of DARP. This problem focuses on optimizing routes for drivers, allowing them to efficiently reach their destinations while accommodating passenger pickups and drop-offs, all within the minimum possible time or cost (Dessouky & Mahtab, 2022). Similarly, in the context of online food delivery, the central system needs to make decisions on how to serve submitted requests by efficiently picking up and delivering orders with the goal of minimizing delivery time, which can be seen as an online variant of DARP (Guo et al., 2022).

A frequently disregarded yet vital aspect in this type of routing problems is the limit on the number of pickups per trip. Many studies tend to focus on constraints such as time windows and maximum ride duration, always assuming these can substitute for pickup limits. Nevertheless, explicitly incorporating restrictions on the number of pickups can be crucial for optimizing delivery operations, especially within the shared mobility sector. For instance, in the context of carpooling, each driver typically accommodates a maximum of four passengers per trip, considering vehicle seat capacity and passenger convenience. Service providers such as UberPool¹, DiDi², and BlaBlaCar³ enforce such restrictions, allowing drivers to pick up no more than two to four passengers on a single trip. Indeed, optimizing a route by initially picking up one passenger and dynamically delivering other passengers, ultimately reaching the first passenger’s destination, is technically feasible. However, private mobility companies often avoid this strategy due to considerations related to passenger comfort. Another influential factor in this consideration is driver preference. In food delivery platforms like Meituan⁴, drivers possess the autonomy to determine the highest number of orders they undertake at one time. Similarly, in the crowdshipping domain, considering drivers’ preferences is crucial as they have the right to set their preferred maximum number for parcel pickups (Arslan et al., 2019). In particular, a company should not anticipate an occasional driver, who might only intend to deliver a few parcels on a sporadic basis or is simply looking to earn some extra income, to handle a high volume of parcels like a full-time staff driver. A similar assumption is found in the concept of limited delivery stops as discussed in Simoni et al. (2020) and Fessler et al. (2022). In this paper, a “customer” can entail more than one person and/or item, but gives rise to only one pickup and two stops (one for pickup and one for delivery).

¹<https://www.uberguide.net/how-many-people-can-ride-in-an-uber/>

²<https://web.didiglobal.com/au/help-center/how-many-people-are-allowed-on-a-didi-share-ride/>

³<https://support.blablacar.com/hc/en-gb/articles/360014470360>

⁴<https://finance.sina.com.cn/tech/2022-05-10/doc-imcwipii9054944.shtml>

In summary, although most previous research has ignored explicit limitations on the number of pickups per trip, in reality such limits have a significant impact on improving customer satisfaction and accommodating driver’s preference. To address such a carpooling scenario where a fleet of vehicles needs to pick up and deliver a group of passengers with the goal to minimize cost, and each vehicle has its unique origin and destination and adheres to a maximum customer pickup limit, this paper introduces an innovative problem termed the Multi-depot Dial-a-Ride Problem with Limited Pickups per Trip (MDARP-LPT). We also introduce a variant called the Dial-a-Ride Problem with Limited Pickups per Trip (DARP-LPT), where all vehicles start and end their routes at the same depot. DARP-LPT is applicable in crowdshipping scenarios, where several occasional riders are used to handle pickup and delivery orders, such as food or parcel deliveries. These riders (e.g. students or part-time riders) do not have specific origins and destinations for travel; their goal is to complete a limited number of orders as a part-time job for additional income. Unlike carpooling, food and parcel deliveries typically occur within a specific physical area, which is why the problem assumes the use of a central depot.

Since MDARP-LPT and DARP-LPT share the same problem structure, we collectively refer to them as (M)DARP-LPT. To efficiently address (M)DARP-LPT, we propose a unified method with two innovative components: fragment-based formulations and novel fragment generation procedures. Firstly, we tailor the fragment-based formulation of DARP proposed by Rist & Forbes (2021) to accommodate (M)DARP-LPT by modifying the decision variables from the fragment-based format to the fragment-vehicle-based format. This change is also necessary for DARP-LPT, where all homogeneous vehicles start and end at the same depot. Secondly, considering the limited number of pickups, we introduce two novel fragment generation procedures. These procedures create improved fragment sets, enhancing computational efficiency. Traditionally, there are two fragment sets: one with longer partial paths and the other with shorter ones. Our two proposed sets diverge: the first refines the fragment set with longer partial paths through path enumeration, while the second blends longer and shorter partial paths from both traditional fragment sets.

From a practical perspective, this research addresses a commonly overlooked aspect in the dial-a-ride problem: the limited number of pickups per trip. Our developed method offers more tailored and efficient solutions for the problem, thereby contributing to the improvement of carpooling and crowdshipping services. From an academic perspective, this study compares and evaluates various fragment sets for the fragment-based formulation in routing problems, providing essential insights for tackling similar pickup and delivery challenges. Furthermore, our innovative fragment generation method accelerates computations

through enumeration; this logic can offer methodological insights for addressing similar routing problems.

The remainder of this article is organized as follows: Section 2 provides a comprehensive literature review. Following that, Section 3 formally defines (M)DARP-LPT, presenting an arc-based formulation and two fragment-based formulations. Section 4 introduces traditional and two novel methods for fragment generation. Then, in Section 5, we analyze the results of our computational experiments. Finally, we draw conclusions in Section 6.

2 Literature review

Since (M)DARP-LPT is a variant of DARP, we investigate existing research methodologies on related optimization problems, such as the Pickup and Delivery Problem (PDP) and the Dial-a-Ride Problem. PDP involves transporting a set of items from their pickup locations to their respective delivery locations (where multiple items from a single pickup node may be destined for different delivery nodes), with the objective of finding optimal routes while minimizing transportation costs (Savelsbergh & Sol, 1995). DARP is a special case of PDP where each location corresponds to a single item, and every item is associated with a unique pickup and delivery location pair.

Traditional methods, like branch and cut (Cordeau, 2006) and branch and price (Ropke & Cordeau, 2009; Baldacci et al., 2011), have been utilized for PDP and DARP, but recent studies suggest that fragment-based methods exhibit better performance. Here, a fragment is a partial path where only the start and end node have an empty load.

A notable example of the fragment-based approach is the work of Alyasiry et al. (2019), who apply a fragment-based strategy to address the Pickup and Delivery Problem with Time Windows, following the Last-In-First-Out loading strategy. They employ the symbol sequence “*ppppddd*” to denote a full fragment, with “*p*” representing a pickup node and “*d*” indicating a delivery node (this representation is also adopted below). This notation implies that, within the fragment, the last pickup must precede the first delivery. Alyasiry et al. (2019) enumerate all possible paths by combining fragments, thus leading to a fragment-based formulation on the time-space network.

The fragments’ applicability extends to various related problems, retaining the characteristic of empty-loaded start and end nodes but not limited to the specific “*ppppddd*” structure. Su et al. (2023) effectively compute the minimum excess user ride time in an electric autonomous DARP using the fragment-based method. Additionally, Zhang et al. (2023) tackle a vehicle-customer coordination problem that shares similarities with DARP

but incorporates the flexibility for passengers to move in order to meet their drivers faster. To tackle this problem, they design an algorithm based on the fragment-based time-space network. Their procedure not only achieves effective results, but also demonstrates its value for online DARP.

Building on Alyasiry et al. (2019), Rist & Forbes (2021) propose the use of restricted fragments to address the dial-a-ride problem. Since the full fragments in this problem may have the form “*ppdpdpdd*” (as an illustration that the last pickup does not precede the first delivery, this does not imply a universal pattern), their number would be quite high. Nevertheless, Rist & Forbes find that a full fragment with the form “*ppdpdpdd*” can be decomposed into the restricted fragments “*ppd*” + “*pd*” + “*pdd*”, which start at a pickup node whose predecessor is a delivery node (or depot) and ends at a delivery node whose successor is a pickup node (or depot). Obtaining these restricted fragments involves initially deriving them from fragments conforming to the form “*ppppddd*” (where the last pickup must precede the first delivery) and then applying a dominance rule to minimize their count. By incorporating temporal information into these restricted fragments, they enable a formulation based on a physical network instead of the time-space network.

While recent literature has made significant contributions to fragment-based methods, other methods may be further improved for (M)DARP-LPT. In particular, alternative methods for fragment generation may result in a higher-quality set of fragments, further enhancing computational performance. Moreover, to the best of our knowledge, no study has conducted a comparison of various fragment types or explored the possibility of combining different fragment categories.

3 Problem statement and linear formulations

Both MDARP-LPT and DARP-LPT are extensions of DARP, and their major difference from DARP lies in the limitations on the number of pickups per trip. In this section, we begin by providing a formal problem description of DARP-LPT and a NP-hardness proof in Section 3.1. Subsequently, we present several linear formulations for DARP-LPT: an arc-based formulation in Section 3.2 and two fragment-based formulations in Section 3.3. The arc-based formulation closely resembles the one outlined in Cordeau (2006), except for the constraints on the limited number of pickups. The two fragment-based formulations expand on the framework of Rist & Forbes (2021), transitioning from a formulation using fragment-based decision variables to one employing fragment-vehicle-based variables. This adaptation is tailored to our specific requirements for limited number of pickups. Finally,

in Section 3.4, we introduce MDARP-LPT, illustrating the differences in its definition and formulations as compared to DARP-LPT.

3.1 Problem description

DARP-LPT involves n customers, with each customer i having a unique pickup and delivery location pair represented as $(i, i + n)$, where n is the total number of customers. The pickup and delivery locations can be represented by the sets $P = \{1, 2, \dots, n\}$ and $D = \{n+1, n+2, \dots, 2n\}$, respectively. The location set $N = P \cup D \cup \{0, 2n+1\}$ consists of all pickup and delivery locations, along with the origin depot location 0 and the destination depot location $2n+1$. Each location $i \in P \cup D$ has a specific time window (e_i, l_i) , defining the earliest and latest time a vehicle can arrive at that location. The arc set is denoted by A , including all arcs $(i, j) \in N \times N$ with $i \neq j$, and the cost and time associated with traversing the arc $(i, j) \in A$ are represented by C_{ij} and T_{ij} , respectively. The set of vehicles is represented by V . The load quantity change at location $i \in N$ is expressed as q_i , with $q_0 = q_{2n+1} = 0$ and $q_i = -q_{n+i}$ ($q_i \in \mathbb{N}^+$) for $i \in P$. This quantity represents the customer size, such as the size of an order or the number of passengers. At pickup location $i \in P$, the vehicle adds load q_i , while at delivery location $i + n \in D$, the vehicle reduces load by q_i .

The objective of DARP-LPT is to minimize travel costs while ensuring that at most $|V|$ vehicles are utilized to visit all pickup and delivery locations, starting from the origin depot location 0 and ending at the destination depot location $2n+1$. To achieve this, a constraint is imposed where each pickup location $i \in P$ must be visited by the same vehicle as its corresponding delivery location $i + n \in D$ (pairing constraints), with the pickup location visited before the delivery location (precedence constraints). Moreover, each customer $i \in P$ has a maximum ride time R_i , each location $i \in N$ has its time window, and each vehicle is limited to a capacity of at most Q with its maximum ride time R_0 .

Up to this point, all the statements adhere to the standard DARP framework. However, an important and unique feature in DARP-LPT is that each vehicle is allowed to have at most L number of pickups. Notably, Q and L are distinct and represent different constraints. Q restricts the maximum size of concurrent customer loads within the vehicle, and the concurrent load can both increase and decrease throughout the trip. In contrast, L limits the total number of pickups, which can only increase monotonically.

DARP-LPT is NP-hard. This can be proven by a reduction from the Capacitated Vehicle Routing Problem (CVRP). CVRP involves arranging a route plan using a fleet of

vehicles to visit a set of customers at minimum cost. Each vehicle has a capacity denoted by C (Cornuejols & Harche, 1993; Achuthan et al., 2003). To perform the reduction, in a DARP-LPT instance, we set the maximum number of pickups per trip L equal to the vehicle capacity C and merge each customer's pickup and delivery nodes into a single node. This creates a problem instance equivalent to CVRP, where each merged node represents a customer with unit size and each vehicle has the capacity C equal to L . Since CVRP is known to be NP-hard when $C \geq 3$ (Chen, 2023), this reduction demonstrates that DARP-LPT is also NP-hard. MDARP-LPT can also be proven to be NP-hard using a reduction similar to DARP-LPT.

3.2 Arc-based formulation of DARP-LPT

The arc-based formulation (ABF), as presented below, is the same as that of Cordeau (2006), except for the constraints (13).

The decision variables are as follows:

Table 1: Decision variables of arc-based formulation

Decision variables	Definition
f_{ijv}	= 1, if the arc $(i, j) \in A$ is traversed by vehicle $v \in V$; = 0, otherwise
t_{iv}	the departure time of vehicle v at location $i \in N$
Q_{iv}	the load of vehicle v after visiting $i \in N$

$$\min \sum_{v \in V} \sum_{(i,j) \in A} C_{ij} f_{ijv} \quad (1)$$

$$s.t. \quad \sum_{v \in V} \sum_{j \in N} f_{ijv} = 1 \quad i \in P \quad (2)$$

$$\sum_{j \in N} f_{ijv} = \sum_{j \in N} f_{(i+n)jv} \quad i \in P, v \in V \quad (3)$$

$$\sum_{j \in N} f_{0jv} = 1 \quad v \in V \quad (4)$$

$$\sum_{j \in N} f_{jiv} = \sum_{j \in N} f_{ijv} \quad i \in P \cup D, v \in V \quad (5)$$

$$\sum_{i \in N} f_{i(2n+1)v} = 1 \quad v \in V \quad (6)$$

$$t_{iv} + T_{ij} \leq t_{jv} + M_{ij}(1 - f_{ijv}) \quad (i, j) \in A, v \in V \quad (7)$$

$$e_i \leq t_{iv} \leq l_i \quad i \in N, v \in V \quad (8)$$

$$Q_{iv} + q_j \leq Q_{jv} + W_{ij}(1 - f_{ijv}) \quad (i, j) \in A, v \in V \quad (9)$$

$$\max(0, q_i) \leq Q_{iv} \leq \min(Q, Q + q_i) \quad i \in N, v \in V \quad (10)$$

$$t_{(n+i)v} - t_{iv} \leq R_i \quad i \in P, v \in V \quad (11)$$

$$t_{(2n+1)v} - t_{0v} \leq R_0 \quad v \in V \quad (12)$$

$$\sum_{(i,j) \in A} f_{ijv} \leq 2L + 1 \quad v \in V \quad (13)$$

$$f_{ijv} \in \{0, 1\} \quad (i, j) \in A, v \in V \quad (14)$$

$$t_{iv} \geq 0 \quad i \in N, v \in V \quad (15)$$

$$Q_{iv} \in \mathbb{N} \quad i \in N, v \in V \quad (16)$$

The objective function (1) aims to minimize the total cost of traversing arcs. Constraints (2) and (3) ensure that each pickup location is visited exactly once and that the paired locations are traversed by the same vehicle. Constraints (4) to (6) specify the network flow requirements. Constraints (7) to (10) ensure time and load consistency. Here, $M_{ij} = \max(0, l_i + T_{ij} - e_j)$ and $W_{ij} = \min(Q, Q + q_i)$. Constraints (11) and constraints (12) set the maximum ride time for customers and vehicles. Constraints (13) restrict the maximum number of pickup locations per trip. If the number of pickups on a route is at most L , then the route has at most $2L$ pickup and delivery locations and $2L + 1$ arcs. Constraints (14) to (16) specify the domain of the variables f , t , and Q .

In order to reduce part of the symmetry that is inherent in the formulation, we define $V_f = \{1, 2, \dots, \lceil n/L \rceil\}$ as the fixed set of vehicles that must be used. This definition arises from the observation that, if a vehicle can deliver at most L customers, a minimum of $\lceil n/L \rceil$ vehicles are needed. Therefore, we add $f_{0(2n+1)v} = 0$ for each fixed vehicle $v \in V_f$.

3.3 Fragment-based formulations of DARP-LPT

The framework presented by Rist & Forbes (2021) defines a fragment-based formulation for DARP, which necessitates the inclusion of callbacks to handle rarely violated constraints related to subtour elimination, time windows, and maximum ride time. In the case of DARP, even when multiple vehicles are used, this fragment-based format remains feasible. In this section, our fragment-based formulations build upon the work of Rist & Forbes (2021). However, since DARP-LPT involves frequently violated constraints, in particular the limitations on the number of pickups per trip (per vehicle), we introduce different decision variables, shifting from a fragment-based format to a fragment-vehicle-based format. Consequently, we propose two distinct fragment-based formulations tailored

for multi-vehicle settings: a fragment flow formulation and a fragment assignment formulation. The former assigns a vehicle to each fragment and node arc, while the latter exclusively links a vehicle with each fragment. In particular, the latter formulation draws inspiration from the client-depot assignment formulation in multi-depot routing problems (Bektaş et al., 2020). In our context, the “client” corresponds to the fragment, while the “depot” corresponds to the vehicle.

3.3.1 Preliminaries and notation

In this subsection, we largely follow the definitions of Rist & Forbes (2021).

A *DARP route* is a route $(0, i_1, i_2, \dots, i_K, 2n+1)$ for which at least one feasible schedule exists, which respects the pairing, precedence, capacity, and time window constraints of DARP. The sequence of locations (i_1, i_2, \dots, i_K) , excluding depot locations, is called a *DARP route path*. Any segment of this sequence is referred to as a route path.

Rist & Forbes (2021) introduce the concept of restricted fragments for DARP. These fragments can be combined to enumerate all DARP routes, and a network is constructed to include all these restricted fragments. Prior to introducing restricted fragments, we describe a full fragment in more detail.

A *full fragment* (FF) refers to a partial DARP route path where only the start and end nodes have an empty load. For instance, a valid fragment could have a sequence of locations $(p1, p2, d2, d1)$ or $(p1, p2, d1, p3, d2, d3)$, where p_j and d_j respectively denote the pickup and delivery locations for customer j . An invalid case is $(p1, d1, p2, p3, d2, d3)$ as this violates the empty load condition after location $d1$ and should be decomposed into $(p1, d1)$ and $(p2, p3, d2, d3)$.

A *restricted fragment* (RF) is a part of a full fragment, starting at a pickup node whose predecessor is a delivery node or depot and ending at a delivery node whose successor is a pickup node or depot. An RF contains at least one pickup-to-delivery movement (not necessarily corresponding to a customer’s pickup and delivery location pair) and cannot be divided into smaller RFs (meaning each RF is as small as possible), e.g., $(p1, p2, d1)$, $(p1, d2, d1)$, $(p1, p2, p3, d4, d5)$, $(p5, d8)$, $(p5, p7, d1, d2, d3)$. The following two examples are not RFs: $(p1, p2, p3, p4)$ and $(p2, d1, p3, d3, d2)$, where the former lacks a pickup-to-delivery movement and the latter can be split after $d1$. A special type of RF is a FF with the format “*ppppdddd*”, where all pickups precede deliveries, and which cannot be divided into smaller RFs, for instance $(p1, p2, d1, d2)$ or $(p1, p3, p2, d2, d1, d3)$. Below are two further examples, where the left-hand side of the equality is the route path of an FF, and the right-hand side consists of RFs. This decomposition is entirely unique.

$$(p2, p1, d2, p4, d4, p3, d1, d3) = (p2, p1, d2) + (p4, d4) + (p3, d1, d3);$$

$$(p2, p5, d2, p4, d4, p3, d5, d3) = (p2, p5, d2) + (p4, d4) + (p3, d5, d3).$$

When combining RFs into routes, it will be crucial to track loads on board. In the first example, the load after visiting locations $d2$ and $d4$ is l_1 , while in the second example, the load after visiting these locations is l_5 , where l_j denotes the load for customer j . This difference highlights that both the route path and the load information are essential for accurately representing an RF. A more precise definition for fragments (RF and FF) will be provided after the introduction of the following concepts.

A *node* is a pair consisting of a location and a set of loads (with customer identification and not just the number of customers) on board, denoted as $(loc(i), loadset(i))$ (or just $loc(i)$ if $loadset(i) = \emptyset$). The $loadset(i)$ includes the unserved customers along a path after departing from location $loc(i)$ but excludes those from $loc(i)$. For instance, the nodes from the route path $(p1, p2, d1, p3, d2, p4, d3, d4)$ are expressed as $p1$, $(p2, \{l_1\})$, $(d1, \{l_2\})$, $(p3, \{l_2\})$, $(d2, \{l_3\})$, $(p4, \{l_3\})$, $(d3, \{l_4\})$, and $d4$. Notably, nodes with the same location can be distinct, as illustrated by examples such as $(p2, \{l_1\})$, $(p2, \{l_3\})$, $(p2, \{l_2, l_3\})$, and $p2$. We define a node with a pickup location as a “pickup node” and a node with a delivery location as a “delivery node”. Specifically, we denote the sets of pickup and delivery nodes as P_N and D_N , respectively, distinguishing them from the sets of pickup and delivery locations denoted as P and D .

A *fragment* (FF and RF) is defined as a partial DARP route path with distinct start and end nodes. The route path records the sequence of locations traversed by a fragment, while the start and end nodes include information regarding the loads onboard. For a FF, merely the route path suffices for reference, while for an RF, alongside the route path, inclusion of both the start and end nodes is necessary for identification. For illustrative purposes, we present several example fragments: $p4 - (p4, d4) - d4$, $(p4, \{l_1\}) - (p4, d4) - (d4, \{l_1\})$, $(p4, \{l_2\}) - (p4, d4) - (d4, \{l_2\})$, $(p4, \{l_1, l_2\}) - (p4, d4) - (d4, \{l_1, l_2\})$. In this context and below, for such a format, the first and last element represent the start and end nodes of the fragment respectively, while the part between two hyphens denotes the route path. Despite following the same route path, these fragments are not the same.

3.3.2 Fragment-based network

Building upon the introductory concepts, we now introduce the fragment-based network. To facilitate comprehension, we present several figures (Fig. 1, Fig. 2, and Fig. 3). In these figures, ellipses represent nodes, solid lines (with ellipses on both sides) indicate fragments (with their route paths written above or to the right), and dashed lines with

arrows are node arcs (further explained below). O^+ and O^- denote the origin depot and destination depot, respectively.

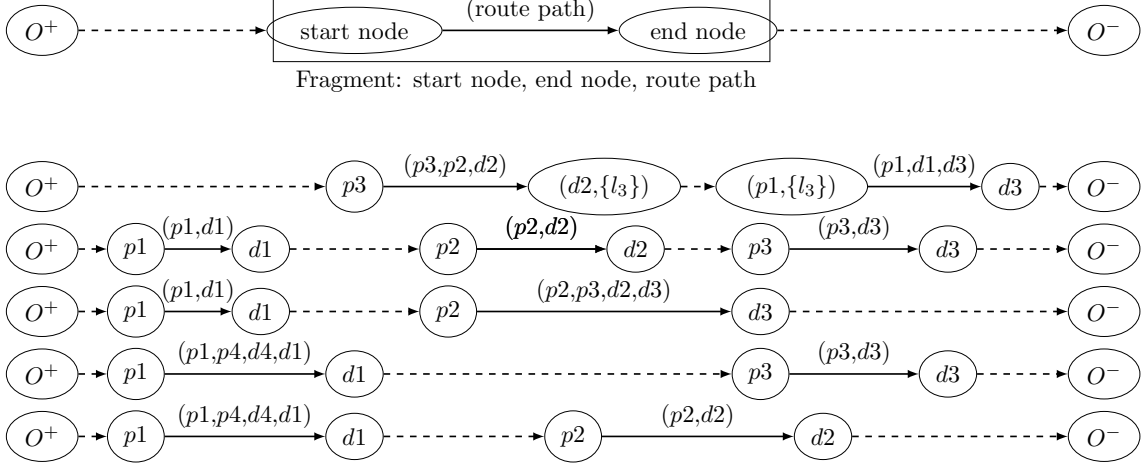


Figure 1: Several feasible routes for DARP and their decomposition into fragments (RF and FF)

Before explaining the fragment-based network, we will introduce the *connections between fragments* and the *connections between nodes* (referred to later as node arcs), both of which can be seen as the dashed lines in Fig. 1. In the former category, the connections between FFs are straightforward. For example: $p1 - (p1, d1) - d1$ can connect to $p2 - (p2, p3, d2, d3) - d3$ to form a route path $(p1, d1, p2, p3, d2, d3)$. However, the connections between RFs require ensuring consistency between the last node's load of the preceding fragment and the first node's load of the succeeding one. Take the following three RFs as an example.

$$\begin{aligned}
 & p2 - (p2, p1, d2) - (d2, \{l_1\}), \\
 & (p4, \{l_1\}) - (p4, d1) - (d1, \{l_4\}), \\
 & (p3, \{l_4\}) - (p3, d4, d3) - d3.
 \end{aligned}$$

These can be combined to a route path $(p2, p1, d2, p4, d1, p3, d4, d3)$. However, the first RF cannot connect to the third one since the load of the end node of the first RF is not the same as that of the start node of the third one.

The connection between two fragments can be indicated by the connection between the preceding fragment's end node and the succeeding fragment's start node. For instance, in the third row of Fig. 1, the connection between $p1 - (p1, d1) - d1$ and $p2 - (p2, d2) - d2$ can be regarded as the connection between $d1$ and $p2$. Furthermore, the connections between

distinct fragments sharing identical end nodes h^- and different fragments with identical start nodes h^+ , can be consistently depicted by the connection (h^-, h^+) . For instance, in the third and fourth row of Fig. 1, the connections between $p1 - (p1, d1) - d1$ and $p2 - (p2, d2) - d2$, as well as between $p1 - (p1, d1) - d1$ and $p2 - (p2, p3, d2, d3) - d3$, can both be represented by the connection $(d1, p2)$.

Therefore, we introduce the concept of *node arc* to describe such a connection between nodes. In the node arc (h^-, h^+) , h^- and h^+ then represent the start and end nodes of the node arc, respectively. This node arc concept differs from the arc concept defined in Section 3.2, as node arcs connect one node to another, with each node encompassing both location and load information (unless the node has empty loads). An additional note is that a node arc can only represent a connection from a delivery node or the origin depot to a pickup node or from a delivery node to the destination depot. This is because all fragments' end nodes must be delivery nodes, while their start nodes must be pickup nodes. Crucially, the connected nodes must share the same load.

Decomposing feasible DARP routes into fragments yields a significantly smaller number of fragments compared to DARP routes. Conversely, if we combine these fragments, we can obtain all feasible DARP routes, albeit with the possibility of some redundant routes. Fig. 2 illustrates how feasible DARP routes can be gathered in a transitional network (as an intermediate step towards the fragment-based network). Fig. 1 presents several DARP routes and their corresponding fragments. The network in Fig. 2 will use these fragments and allow to enumerate all the DARP routes shown in Fig. 1. Identical fragments across different routes in Fig. 1 can be consolidated into a single fragment while maintaining the connections to other fragments. Subsequently, the fragment-based network of Fig. 3 is derived from the network of Fig. 2. When different fragments share the same start and/or end nodes, then those nodes can also be merged. For instance, two fragments with the same start and end nodes but different route paths $(p1, d1)$ and $(p1, p4, d4, d1)$ become two route paths originating from node $p1$ and terminating at node $d1$. Such consolidations help reduce connections (node arcs). Node arcs with the same start node and end node can also be merged; the three connections from $(p1, d1)$ to $(p2, d2)$, from $(p1, d1)$ to $(p2, p3, d2, d3)$, and from $(p1, p4, d4, d1)$ to $(p2, d2)$ in Fig. 2, for instance, can be merged into one node arc $(d1, p2)$ in Fig. 3.

The practical process of network generation proceeds as follows. The fragment-based network comprises nodes, fragments, and node arcs. The initial step involves generating fragments (outlined in Section 4). Following this, the start and end nodes of all fragments are identified and added to the network. Subsequently, all fragments are integrated into

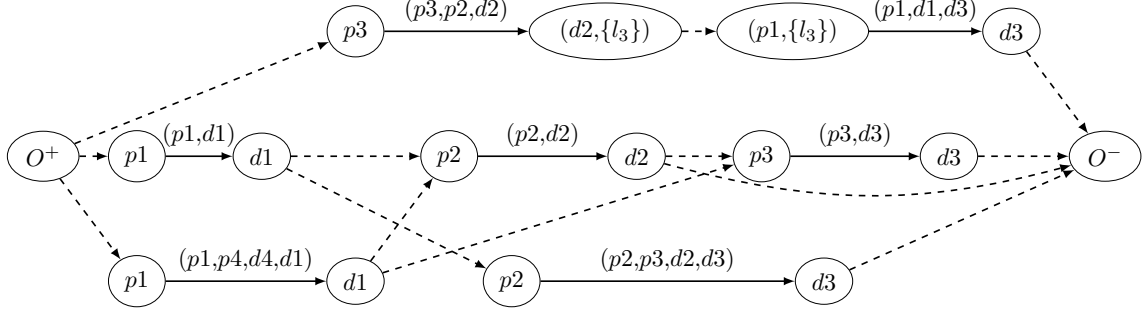


Figure 2: A transitional network for DARP by merging all identical fragments from Fig. 1

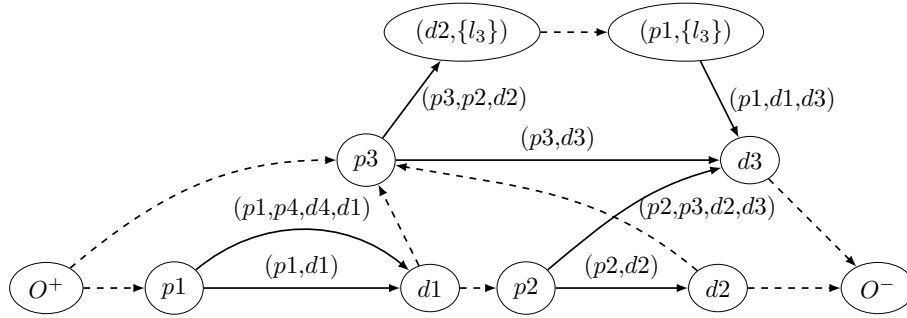


Figure 3: Fragment-based network for DARP by merging all identical nodes from Fig. 2

the network, connecting from their start nodes to end nodes. Different fragments can share the same start and/or end nodes. In the final phase, for the node arcs, all delivery nodes and the origin depot connect with all pickup nodes, and all delivery nodes connect with the destination depot. If none of the fragments ending at h^- can connect to any fragment starting at h^+ due to time window or any other constraints, the node arc (h^-, h^+) can be eliminated. When the network exclusively includes FFs, the number of node arcs (excluding those involving depots) is at most $|n| \times |n|$. For the network with RFs, the potential number of node arcs could be higher due to the possibility of different nodes with the same location having different loads. Moreover, a feasible route typically starts with a node arc from the depot, followed by a fragment leading to a delivery node. Subsequently, there must be a node arc from the current delivery node to another pickup node or the destination depot. After that, if the current node is not the depot yet, it must be succeeded by another fragment and then a node arc again, continuing in this pattern. Therefore, any feasible route in Fig. 3 must adhere to the alternating pattern of dashed lines and solid lines.

We now formalize the foregoing concepts. The set of *nodes* is expressed as: $N_N =$

$P_N \cup D_N \cup \{O^+, O^-\}$, where the origin depot O^+ and destination depot O^- correspond to location 0 and location $2n + 1$, respectively. The set of fragments, denoted as F , is derived from customer locations, as detailed in Section 4. F may include both FFs and RFs or exclusively one type. We use the notation F_h^+ for the sets of fragments starting at pickup node $h \in P_N$, F_h^- for those ending at delivery node $h \in D_N$, and F_i for the set of fragments traversing location $i \in P \cup D$. Additionally, A_N , A_n^+ , and A_n^- represent the set of node arcs, the set of node arcs starting from delivery node (or the origin depot) $h \in D_N \cup \{O^+\}$, and the set of node arcs ending at pickup nodes (or the destination depot) $h \in P_N \cup \{O^-\}$, respectively. Notably, A_N exclusively includes node arcs originating from delivery nodes (or the origin depot) and terminating at pickup nodes (or the destination depot).

For each fragment $f \in F$, we designate the number of included pickup nodes as L_f , and its cost c_f is calculated as the sum of travel costs over all locations visited by the fragment, i.e., $c_f = \sum_{(i,j) \in f} C_{loc(i)loc(j)}$, where $loc(i)$ represents the location of node $i \in N_N$. Furthermore, the cost of node arc a , c_a , is determined as follows: $c_a = C_{loc(i)loc(j)}$, $a = (i, j)$, $a \in A_N$.

3.3.3 Fragment flow formulation

The first fragment-based formulation is the *fragment flow formulation* (FFF), which expands on the framework of Rist & Forbes (2021). It transitions from a formulation using fragment-based and node arc-based decision variables to one employing fragment-vehicle-based and node arc-vehicle-based variables. Please note that the current formulation below is not complete. Lazy constraints, specifically designed for the elimination of infeasible paths, are applied to address subtour elimination, time windows, and maximum ride time. The details are described in Section 3.3.6.

Table 2: Decision variables of FFF

Decision variables	Definition
x_{fv}	= 1, if fragment $f \in F$ is traversed by vehicle $v \in V$; = 0, otherwise
y_{av}	= 1, if node arc $a \in A_N$ is traversed by vehicle $v \in V$; = 0, otherwise

$$\min \sum_{v \in V} \sum_{f \in F} c_f x_{fv} + \sum_{v \in V} \sum_{a \in A_N} c_a y_{av} \quad (17)$$

$$s.t. \quad \sum_{f \in F_h^-} x_{fv} = \sum_{a \in A_h^+} y_{av} \quad h \in P_N, v \in V \quad (18)$$

$$\sum_{f \in F_h^+} x_{fv} = \sum_{a \in A_h^-} y_{av} \quad h \in D_N, v \in V \quad (19)$$

$$\sum_{v \in V} \sum_{f \in F_i} x_{fv} = 1 \quad i \in P \quad (20)$$

$$\sum_{f \in F} L_f x_{fv} \leq L \quad v \in V \quad (21)$$

$$x_{fv}, y_{av} \in \{0, 1\} \quad f \in F, a \in A_N, v \in V \quad (22)$$

The objective function (17) minimizes the weighted cost of used fragments and node arcs. Constraints (18) and (19) describe the network flow for fragments and node arcs. For each pickup node at which a fragment ends, there must be a node arc starting from it. Similarly, for each delivery node at which a fragment starts, a node arc must end at that node. These relationships are applicable to each vehicle. Constraints (20) guarantee that each pickup location is visited exactly once. Constraints (21) set the maximal number of pickups. Constraints (22) specify the domains of x and y .

The additional constraints (23) below specify whether a vehicle is used or unused. They are not necessary but can assist the solver in branching, and thus, improve computational performance. Here, we define w_v as 1 if vehicle $v \in V$ is utilized, and 0 otherwise.

$$\sum_{a \in A_{O+}^+} y_{av} = w_v \quad v \in V \quad (23)$$

3.3.4 Fragment assignment formulation

Table 3: Decision variables of FAF

Decision variables	Definition
X_f	= 1, if fragment $f \in F$ is traversed; = 0, otherwise
Y_a	= 1, if node arc $a \in A_N$ is traversed; = 0, otherwise
x_{fv}	= 1, if fragment $f \in F$ is traversed by vehicle $v \in V$; = 0, otherwise

An alternative formulation involves the assignment of fragments to vehicles and is called *fragment assignment formulation* (FAF). FAF extends the framework of Rist & Forbes

(2021) by transitioning from a formulation using fragment-based decision variables to one that incorporates fragment-vehicle-based variables. Unlike FFF, however, which introduces node arc-vehicle-based decision variables, FAF keeps the node arc-based variables by means of a separate set of constraints (which hinges upon constraint set (31)). This model is inspired by the client-depot assignment formulation used in multi-depot routing problems (Bektaş et al., 2020). In the same way as for FFF, the current formulation below is not complete. Lazy constraints to address subtour elimination, time windows, and maximum ride time are discussed in Section 3.3.6.

$$\min \sum_{f \in F} c_f X_f + \sum_{a \in A_N} c_a Y_a \quad (24)$$

$$s.t. \quad \sum_{f \in F_h^-} X_f = \sum_{a \in A_h^+} Y_a \quad h \in P_N \quad (25)$$

$$\sum_{f \in F_h^+} X_f = \sum_{a \in A_h^-} Y_a \quad h \in D_N \quad (26)$$

$$\sum_{f \in F_i} X_f = 1 \quad i \in P \quad (27)$$

$$\sum_{a \in A_{O^+}^+} Y_a \leq |V| \quad (28)$$

$$x_{fv} \leq X_f \quad f \in F, v \in V \quad (29)$$

$$\sum_{v \in V} x_{fv} = X_f \quad f \in F \quad (30)$$

$$\sum_{f \in F_i^-} x_{fv} + Y_a \leq \sum_{f \in F_j^+} x_{fv} + 1 \quad a = (i, j) \in A_N : i \neq O^+, j \neq O^-, v \in V \quad (31)$$

$$\sum_{f \in F} L_f x_{fv} \leq L \quad v \in V \quad (32)$$

$$X_f, Y_a \in \{0, 1\} \quad f \in F, a \in A_N \quad (33)$$

$$x_{fv} \in \{0, 1\} \quad f \in F, v \in V \quad (34)$$

The objective function (24) minimizes the weighted cost of used fragments and node arcs. Constraints (25) and (26) describe the network flow for fragments and node arcs. Constraints (27) guarantee that each pickup location is visited exactly once. Constraints (28)

state that at most $|V|$ vehicles are used. Constraints (29)-(31) assign the fragments to vehicles. Specifically, constraints (29) impose that if a fragment is traversed by a vehicle, the fragment is used; constraints (30) state that if a fragment is chosen, it must be assigned to a vehicle; and constraints (31) express that if a node arc is used, the fragments preceding the arc and the fragments succeeding the arc must be traversed by the same vehicle. This explains why it does not matter which vehicle traverses the node arc. Constraints (32) set the maximal number of pickups. Constraints (33) and constraints (34) specify the domains of X , Y , and x .

Although the variables X and x in this formulation can be expressed solely in terms of x , keeping both X and x yields better computational results.

3.3.5 Comparison of FFF and FAF

In this subsection, we will establish that FFF is a stronger formulation than FAF. We will show this in two steps. Firstly, any feasible solution to the linear relaxation of FFF also qualifies as a feasible solution to the linear relaxation of FAF. Secondly, we will provide an example solution from the polytope of FAF that does not appear in the polytope of FFF.

Regarding the first step, it is easy to observe that constraints (18)-(20) and constraints (21) in FFF can imply constraints (25)-(27) and constraints (32) in FAF. Furthermore, constraints (23) in FFF can indicate constraints (28) in FAF. Therefore, our only task is to demonstrate how a solution (x', y') that is feasible under FFF constraints (18) and (19) can meet the requirements of FAF constraints (31). Let (x', y') represent a solution from the linear relaxation of FFF. We introduce two auxiliary variables: X' and Y' . Here, $X'_f = \sum_{v \in V} x_{fv}$ for all $f \in F$ and $v \in V$; and $Y'_f = \sum_{v \in V} y'_{av}$ for all $a \in A_N$ and $v \in V$.

Proposition 1. *Constraints (18) and constraints (19) in FFF imply constraints (31) in FAF.*

Proof. Consider an arc $a = (i, j)$. Our objective is to demonstrate that any solution (x', y', X', Y') satisfying the FFF constraints will also be feasible for the FAF network flow constraints (31).

According to the FFF network flow constraints (18) and (19), we have:

$$\sum_{f \in F_i^-} x'_{fv} = \sum_{a \in A_i^+} y'_{av}, \quad \text{and} \quad \sum_{f \in F_j^+} x'_{fv} = \sum_{a \in A_j^-} y'_{av}$$

Thus, we can transform the FAF constraints (31) as follows:

$$\sum_{f \in F_i^-} x'_{fv} + Y'_a \leq \sum_{f \in F_j^+} x'_{fv} + 1 \iff \sum_{a' \in A_i^+} y'_{a'v} + Y'_a \leq \sum_{a' \in A_j^-} y'_{a'v} + 1 \iff \sum_{a' \in A_i^+ \setminus a} y'_{a'v} + Y'_a \leq \sum_{a' \in A_j^- \setminus a} y'_{a'v} + 1$$

We now examine the left side of the last inequality, $\sum_{a' \in A_i^+ \setminus a} y'_{a'v} + Y'_a$, using FFF constraints (18). Then, we obtain:

$$\sum_{a' \in A_i^+ \setminus a} y'_{a'v} + Y'_a \leq \sum_{a \in A_i^+} Y_a = \sum_{f \in F_i^-} X_f \leq 1 \leq \sum_{a' \in A_j^- \setminus a} y'_{a'v} + 1$$

Thus, we see that constraints (31) are automatically fulfilled if constraints (18) and (19) hold. \square

The second step is to show that the polyhedra of the two formulations do not coincide. To illustrate this point, we provide an example solution of FAF that is cut away by FFF. For example: if $V = \{v1, v2\}$, $F_i^- = \{f\}$, $F_j^+ = \{g\}$, and $a = (i, j)$, constraints (31) of FAF become: $x_{fv1} + x_{fv2} + Y_a \leq x_{gv1} + x_{gv2} + 1$. A potential solution under the given constraints is $x_{fv1} = 0.5$, $x_{fv2} = 0.5$, $Y_a = 1$, $x_{gv1} = 1$, $x_{gv2} = 0$. However, this solution does not satisfy constraints (18) and (19) of FFF, where $x_{fv2} = y_{av2}$ and $y_{av2} = x_{gv2}$.

Based on the foregoing, we conclude that FFF dominates FAF. Despite this dominance result, we should still verify empirically how the two formulations behave in terms of run-times. FAF, for instance, has less decision variables since FAF utilizes arc-based variables Y , whereas FFF uses arc-vehicle-based variables y .

3.3.6 Inequalities for fragment formulations

The above fragment-based formulations FFF and FAF may not be sufficient to lead to feasible solutions. Subtour elimination, time windows, and maximum ride time constraints will be implemented by the callbacks of infeasible path constraints, in line with Alyasiry et al. (2019); Rist & Forbes (2021). The details are as follows. As long as we encounter an incumbent solution in the branch-and-bound tree, we create chains or cycles. A *chain* is a sequence of fragments (f_1, \dots, f_c) with a fragment count of $c > 1$, along with $c - 1$ node arcs (a_1, \dots, a_{c-1}) connecting them. The load of the end node of fragment f_i must be the same as that of the start node of f_{i+1} for $1 \leq i \leq c - 1$; the start node and the end node of a_i correspond to the end node of fragment f_i and the start node of f_{i+1} , respectively, for $1 \leq i \leq c - 1$. Similarly, a *cycle* is a sequence of fragments (f_1, \dots, f_c) with

a fragment count of $c > 1$, along with c node arcs (a_1, \dots, a_c) connecting them. A cycle has the same connection requirement as a chain but includes an additional node arc a_c that connects f_c back to f_1 . If we obtain a chain, we connect its initial and final fragments to the origin and destination depots, respectively, to construct a path. After that, we establish a valid time schedule for the path, following the constraints of time windows and maximum ride time. If no valid schedule can be found, the chain is considered infeasible and then needs to be eliminated by constraints (35), which ensures that the total count of fragments and node arcs in such a chain does not exceed $2c - 2$. If a cycle is detected, we then remove it using constraints (36) to ensure that the total count of its elements does not exceed $2c - 1$, thereby achieving subtour elimination. While callbacks are a useful approach for rarely violated constraints, like the constraints mentioned above, they are not ideal for constraints that are easily violated, such as the limit on the number of pickups.

$$\sum_{k=1}^c x_{f_k v} + \sum_{k=1}^{c-1} y_{a_k v} \leq 2c - 2 \quad v \in V \quad (35)$$

$$\sum_{k=1}^c x_{f_k v} + \sum_{k=1}^c y_{a_k v} \leq 2c - 1 \quad v \in V \quad (36)$$

In addition to the necessary constraints mentioned earlier, we incorporate three types of inequalities proposed by Rist & Forbes (2021), namely fragment-fragment, arc-fragment, and fragment-arc inequalities, and add the subset-row inequalities proposed by Jepsen et al. (2008). Fragment-fragment inequalities stipulate that when a fragment is traversed, at least one fragment from its preceding and one fragment from its succeeding fragment set must also be traversed. The preceding and succeeding fragment sets include all fragments except the ones that, when combined with the current fragment, would result in infeasible paths. Arc-fragment inequalities state that if a node arc is traversed, at least one fragment from its succeeding and one fragment from its preceding fragment set must be traversed to maintain path feasibility. Fragment-arc inequalities specify that if a fragment is traversed, at least one succeeding node arc and one preceding node arc in the corresponding sets must also be traversed. In addition, for subset-row inequalities, we follow the same approach as Rist & Forbes (2021) and Jepsen et al. (2008).

Furthermore, to enhance the formulations (both FFF and FAF), we introduce additional constraints based on the minimum number of used vehicles, as shown in constraints (37).

While these constraints may be redundant, they significantly speed up the computation process. Additionally, for constraints (23), we set w_v equal to 1 for $v \in V_f$.

$$\sum_{f \in F} x_{vf} \geq 1 \quad v \in V_f \quad (37)$$

3.4 MDARP-LPT: problem description and formulations

The primary distinction between MDARP-LPT and DARP-LPT lies in the fact that in DARP-LPT all drivers must initiate their journeys from the origin depot O^+ and return to the destination depot O^- . Conversely, in MDARP-LPT, each vehicle $v \in V$ possesses its own unique origin location o_v and destination location d_v (denoted as O_v and D_v for origin and destination nodes, respectively). In all other aspects, MDARP-LPT adheres to the same principles as DARP-LPT.

The formulations developed supra (ABF, FFF, and FAF) for DARP-LPT can also be used for MDARP-LPT, with some modifications as explained below.

For ABF, only the network flow constraints (4)-(6) need to be updated to reflect the unique origin and destination for each vehicle. The complete formulation can be found in A.

For FFF, all constraints (18)-(22) remain applicable, but the network configuration assigns unique origin and destination nodes, fragment sets, node arc sets, and node sets to each vehicle.

For FAF, in addition to the network adjustments, two further constraints, constraints (38) and (39), must be incorporated. These constraints stipulate that when a node arc starting from an origin is utilized, the subsequent fragments must also be employed, and similarly, when a node arc ending at a destination is employed, the preceding fragments must also be utilized. Specifically, for each vehicle, it possesses a unique set of node arcs that originate from its origin and a unique set of node arcs that end at its destination node.

$$Y_a \leq \sum_{f \in F_j^+} x_{fv} \quad a = (O_v, j) \in A_N, v \in V \quad (38)$$

$$Y_a \leq \sum_{f \in F_j^-} x_{fv} \quad a = (j, D_v) \in A_N, v \in V \quad (39)$$

Additionally, for both FFF and FAF, the model for MDARP-LPT needs to incorporate infeasible path constraints (constraints (35)) through callback procedures to handle the constraints of subtour elimination, time windows, and maximum ride time. Given that MDARP-LPT involves distinct vehicles with unique origins and destinations, constraints such as (37) based on the minimum number of vehicles are not used for MDARP-LPT.

4 Fragment generation

In this section we describe how the fragments that constitute the basis for the formulations FFF and FAF can be acquired. Section 4.1 describes the FF generation procedure of Alyasiry et al. (2019) and the RF generation method of Rist & Forbes (2021), both of which involve enumeration. The resulting fragment sets for (M)DARP-LPT are denoted as S_{FF} and S_{RF} , respectively. From these sets, all fragments whose length exceeds L are already eliminated. The set S_{FF} with longer fragments tends to be larger than S_{RF} with shorter fragments, yet all combinations of RFs from S_{RF} can generate more (redundant) FFs than those in S_{FF} .

In DARP, solution paths can vary in length, potentially exceeding L . However, in (M)DARP-LPT, solution paths must not exceed this limit. Since S_{FF} and S_{RF} are primarily designed for DARP, some of their fragments (even if not exceeding L in length) might only appear on solution paths that exceed L and not on those that adhere to the limit (because some higher-cost paths are eliminated from consideration; see Section 4.2). Therefore, in Section 4.2, we introduce a novel path-enumerated full fragment set S_{PFF} by enumerating all (M)DARP-LPT paths first and then decomposing them into full fragments. Consequently, S_{PFF} must be a subset of S_{FF} . Another novel method in Section 4.3 is to create a mixed fragment set S_{MF} by converting certain FFs from S_{FF} into RFs while keeping others, aiming to leverage the strength of both FFs and RFs and potentially reduce the set size.

All these fragment sets (S_{FF} , S_{RF} , S_{PFF} , and S_{MF}) are valid for both MDARP-LPT and DARP-LPT. However, in MDARP-LPT, where vehicles have different origins and destinations, each vehicle requires a unique fragment set (though many of the fragments will still be the same for each vehicle). Therefore, the generation procedure for MDARP-LPT must be executed $|V|$ times, where $|V|$ denotes the number of vehicles. In contrast, DARP-LPT, with a fixed depot for all vehicles, only necessitates a single execution of the generation procedure.

4.1 Traditional fragment generation

Alyasiry et al. (2019) introduce FF and S_{FF} , while Rist & Forbes (2021) propose RF and S_{RF} . S_{FF} exclusively contains FFs, while S_{RF} exclusively contains RFs. Their intersection includes all FFs with the format “ $ppppdddd$ ”, which can also be regarded as RFs. As previously explained, “ $ppppdddd$ ” indicates a sequence where all pickups precede all deliveries.

The fragment generation procedure of Alyasiry et al. (2019) involves enumerating all FFs that satisfy constraints such as time windows, maximum ride time, pairing, precedence, and capacity limits. In Rist & Forbes (2021), fragment generation is relatively intricate. Although an RF is always a part of at least one FF (see Section 3.3.1), Rist & Forbes do not directly derive RFs from FFs. Instead, they only focus on FFs with the specific format “ $ppppdddd$ ”. These specific FFs are initially enumerated and then partitioned into all possible combinations. For example, $(p1, p2, p3, d1, d2, d3)$ can be partitioned as follows: $(p1, p2, p3, d1, d2, d3)$, $(p1, p2, p3, d1, d2)$, $(p1, p2, p3, d1)$, $(p2, p3, d1, d2, d3)$, $(p2, p3, d1, d2)$, $(p2, p3, d1)$, $(p3, d1, d2, d3)$, $(p3, d1, d2)$, $(p3, d1)$. Building upon the partitioned results, they then systematically enumerate all feasible RFs. An additional step involves transforming a partitioned segment above into an RF. For each segment, the left and right parts (customers) cut from the original FF would contribute to the load set of the start and end nodes of the newly constructed RF, respectively. For example, for the segment $(p3, d1)$, its left side (**p1, p2**) and right side (**d2, d3**) were cut from the original FF (**p1, p2, p3, d1, d2, d3**); then for the newly formed RF, the start node becomes $(p3, \{l_1, l_2\})$ and the end node becomes $(d1, \{l_2, l_3\})$. Hence, the final RF derived from $(p3, d1)$ is $(p3, \{l_1, l_2\}) - (p3, d1) - (d1, \{l_2, l_3\})$. After fragment enumeration, both FF and RF procedures can remove some fragments by applying domination rules that consider time windows and cost; for more details we refer to Rist & Forbes (2021). Finally, it is important to note that the constraints on the maximum number of pickups are integrated into the fragment enumeration process so that the resulting sets S_{FF} and S_{RF} are directly applicable to (M)DARP-LPT. Since both fragment sets are generated by enumerating all possible fragments for (M)DARP-LPT, using these sets in fragment-based formulations can achieve optimality.

4.2 Path-enumerated full fragment generation

Generating S_{PFF} involves three steps: enumerating all paths that adhere to the problem constraints, selecting enumerated paths, and generating fragments from these selected paths. The first step is to enumerate all possible paths. Typically, such a task can be

challenging due to the exponential growth in the number of paths. With limited pickups, however, this number is polynomial for L . To be more precise, the number of paths is bounded by $\mathcal{O}((2n)^{2L})$. The second step involves path selection. For any pair of enumerated paths that visit an identical set of locations, only the one with lower cost is kept. The third step involves extracting full fragments from the selected paths. Within each path, nodes with empty loads are identified and marked. The route paths delimited by consecutive markers are then extracted to create fragments, which are subsequently recorded in S_{PFF} . Notably, S_{PFF} should be a subset of S_{FF} , as S_{PFF} is derived from the selected paths, and not all FFs from S_{FF} will appear on these paths. Since S_{PFF} includes all FFs obtained from all non-dominated (M)DARP-LPT paths (paths with higher cost are excluded), these FFs can also be re-combined to reconstitute all non-dominated paths.

We illustrate the foregoing with an example. Consider an instance with only two customers, 1 and 2. The set S_{FF} includes the following fragments: $(p1, p2, d1, d2)$, $(p1, p2, d2, d1)$, $(p2, p1, d1, d2)$, $(p2, p1, d2, d1)$, $(p1, d1)$, and $(p2, d2)$. However, there are at most three useful paths: $(0, p1, d1, 2n + 1)$, $(0, p2, d2, 2n + 1)$, and then out of the four paths that include the four locations $p1$, $p2$, $d1$, and $d2$ and serve both customers, only one of the four (a shortest path) needs to be retained. As a result, S_{PFF} can contain at most three fragments from the three paths and is thus clearly a subset of S_{FF} .

4.3 Mixed fragment generation

Path enumeration can become significantly more time-consuming as the limit on the number of pickups L increases. Hence, we present an alternative procedure for creating fragments as L grows. In this procedure, we initially create all FFs to get S_{FF} . Next, we employ a selection process to identify specific FFs to be decomposed into RFs. Finally, the remaining FFs together with the newly formed RFs constitute the set S_{MF} .

The first step generates FFs adhering to the (M)DARP-LPT constraints, according to the procedure described in Section 4.1, resulting in the same fragment set S_{FF} .

The second step decomposes all FFs into RFs and records the frequency of occurrence of each RF during this process. In a FF, pickup nodes whose preceding nodes are depots or delivery nodes, and delivery nodes whose subsequent nodes are depots or pickup nodes, are marked. The route paths between consecutive marks can be utilized to create RFs. During the process of obtaining RFs from FFs, we keep track of how frequently each RF appears in all FFs. This work is preparatory for the third step. An important aspect to note is that the resulting full RF set should be a subset of S_{RF} . This can be seen as follows: S_{RF} encompasses all RFs obtained by partitioning FFs with the “ppppdddd”

format in all possible ways. However, some RFs in S_{RF} may never appear in any FF in S_{FF} . Specifically, these RFs might only be combined with specific other RFs to form FFs that are dominated.

The third step involves selecting FFs for decomposition, aiming to create a mixed fragment set comprising both FFs and RFs. The main objective of working with such a mixed set is to reduce the fragment count. An initial assumption is that S_{FF} typically contains more fragments than S_{RF} . Intuitively, decomposing all FFs into RFs might seem beneficial. However, we find that if an FF includes several RFs and these RFs do not appear in any other non-dominated FFs in S_{FF} , decomposing it can increase the total fragment count. Furthermore, our computational results in Section 5.2.1 indicate that when RFs are used in the formulations, they may lead to weaker lower bounds compared to FFs. Based on these two observations, we only decompose a portion of FFs in S_{FF} . Specifically, we maintain a record of how frequently each RF appears in the FFs from the previous step. Only the FFs for which all the constituent RFs appear multiple times (at least three times, in our implementation) within all FFs in S_{FF} are candidates for decomposition. Other FFs that do not meet this criterion are retained in their original form. As a result, the undecomposed FFs together with the RFs obtained through this process constitute S_{MF} . Thus, it can be seen that S_{MF} can serve the same role as S_{FF} in enumerating all (M)DARP-LPT paths and act as the input for formulations without compromising optimality.

5 Computational results

5.1 Data generation and implementation details

To assess computational efficiency of different formulations and fragment sets, we utilize benchmark instances from Cordeau (2006), which are widely adopted in studies such as Ropke et al. (2007); Gschwind & Irnich (2015); Rist & Forbes (2021). These instances comprise two types, A and B, with type A having a tighter maximum ride time. In type A, customer demand is unit with a vehicle capacity of three, while type B involves demands from one to six customers with a vehicle capacity of six.

For DARP-LPT, we generate both basic and extended instances. The basic instances adjust the vehicle numbers $|V|$ in Cordeau’s instances. Given that DARP-LPT incorporates an additional parameter L for the maximal number of pickups per trip, ensuring coverage for n customers requires a minimum of $\lceil n/L \rceil$ vehicles. Here, we set $|V|$ as $\lceil n/(L - 1) \rceil$, which is slightly higher than the minimum required. We also create an extra instance set to

which we refer as “extended” instances, following Gschwind & Irnich, in which we increase time windows and capacity by 1/3 relative to the basic instances, thereby enhancing the diversity of the problem instances.

For MDARP-LPT, which assumes different drivers have distinct origins and destinations, we generate driver information based on Cordeau’s instances. Specifically, the first $\lceil n/\alpha \rceil$ customers are designated as drivers, whose pickup and delivery nodes becoming the origins and destinations, while the remaining customers are passengers. The value n represents the number of customers in each Cordeau instance, and α is an auxiliary parameter. The choice $L = 4$ and $\alpha = 4$ implies that one driver serves three customers on average, and $\alpha = 3$ has one driver per two customers on average. For drivers’ time windows, we set the earliest departure to 0, maintaining latest arrival times. Their maximum ride time is halved from the original driver’s maximum ride time (which is between six and 12 hours), as the latter is excessive for realistic scenarios such as carpooling. Unit customer demand and capacity 4 are chosen.

Table 4 summarizes our experimental design. We use S_{PFF} for MDARP-LPT and S_{MF} for DARP-LPT. This decision is based on the appropriateness of S_{PFF} for low L values, which aligns well with real carpooling scenarios in MDARP-LPT. On the other hand, S_{MF} is used for comparison with S_{RF} and S_{FF} across diverse L values, a context more suitable for DARP-LPT. We do not apply S_{MF} for MDARP-LPT because each vehicle has distinct fragment sets, and mixing the FFs and RFs per vehicle would become overly complex.

Table 4: Experimental design

Problem	Instance	L	$ V $	Customer number	Formulation	Fragment set
DARP-LPT	basic	4, 6	$\lceil n/(L - 1) \rceil$	n	ABF, FAF, FFF	S_{FF}, S_{RF}, S_{MF}
	extended					
MDARP-LPT	basic	4	$\lceil n/\alpha \rceil$	$n - \lceil n/\alpha \rceil$	FFF	S_{FF}, S_{RF}, S_{PFF}

¹ Value n is the number of customers in the original instance of Cordeau (2006).

All our algorithms are implemented using the Python programming language. All computational experiments are run on a system with an Intel Core i7-7820HQ processor with 2.90 GHz CPU speed and 32 GB of RAM under a Windows 10 64-bit OS. All linear formulations are solved with the commercial solver Gurobi 9.0.3 with a single thread; all other Gurobi parameters are set to their default values. The generation of fragments is implemented using the Python programming language. For DARP-LPT, fragment generation occurs in a single-processing environment, whereas for the MDARP-LPT, fragment

generation is accomplished via multi-processing.

Since this study involves two problems (DARP-LPT and MDARP-LPT), two different fragment-based formulations, four types of fragment sets, and two types of instances (basic and extended), we need to test multiple combinations. Therefore, from the existing benchmark instances, we only choose a subset, but we ensure a variety of sizes as indicated by the instance names in all following tables.

5.2 Discussion of the results

In our evaluation of computational performance, we incorporate several performance indicators: time, OBJ, LB, and gap. Time (s) indicates the total time, including the preprocessing time, network time, and CPU time for solver execution. Here, preprocessing time refers to the duration spent on time window tightening and arc elimination, as detailed by Cordeau (2006). Network time refers to the time required for fragment generation and the construction of the fragment-based network. OBJ and LB are the best-found integer solution value and the best lower bound within a 30-minute timeframe, respectively, and gap represents the relative percentage difference between OBJ and LB. When comparing different fragment sets, we also introduce two additional indicators: fragment count and network time. Fragment count is the total number of fragments in the fragment set.

5.2.1 Results for DARP-LPT

Table 5 compares the three formulations ABF, FAF, and FFF for DARP-LPT for a runtime limit of 30 minutes, using the basic instances with the parameters $|V| = \lceil n/3 \rceil$ and $L = 4$. Both FAF and FFF utilize S_{FF} as the input fragment set. The table indicates that, as observed from the time and gap indicators, both FFF and FAF largely outperform ABF, with FFF exhibiting superior performance compared to FAF.

Table 5: Computational performance of different formulations for DARP-LPT within 30 minutes

		ABF			FAF (S_{FF})				FFF (S_{FF})			
Name	Time (s)	OBJ	LB	Gap	Time (s)	OBJ	LB	Gap	Time (s)	OBJ	LB	Gap
a3-18	24.3	302.5	302.5	0.00%	0.2	302.5	302.5	0.00%	0.2	302.5	302.5	0.00%
a3-30	1800.0	496.7	451.2	9.16%	1800.0	494.8	491.6	0.64%	1800.0	494.8	491.1	0.74%
a3-36	1800.0	574.4	541.2	5.78%	1800.0	574.4	565.9	1.49%	1800.0	574.4	565.0	1.63%
a4-48	1800.0	712.0	578.3	18.78%	1800.0	698.6	685.4	1.90%	1800.0	697.9	687.4	1.50%
a6-60	1800.0	920.2	635.4	30.95%	1800.0	879.2	843.2	4.09%	1800.0	864.9	843.4	2.48%
a7-70	1800.0	1284.3	664.6	48.25%	1800.0	1004.0	958.2	4.56%	1800.0	986.6	956.5	3.05%
a8-80	1800.0	1359.6	670.4	50.69%	1800.0	1100.7	1017.9	7.53%	1800.0	1071.1	1019.3	4.84%
Avg-A	1546.3			23.37%	1542.9			2.89%	1542.9			2.03%
b3-36	1800.0	576.5	548.4	4.88%	1800.0	576.5	566.8	1.69%	1800.0	576.5	567.7	1.53%
b4-40	1800.0	637.5	612.5	3.92%	1800.0	635.2	630.2	0.79%	1800.0	635.2	631.1	0.64%
b5-50	1800.0	796.5	659.3	17.22%	1800.0	798.4	765.7	4.10%	1800.0	789.1	768.3	2.63%
b6-60	1800.0	937.9	749.9	20.05%	1800.0	940.6	896.5	4.68%	1800.0	931.7	900.7	3.33%
b7-70	1800.0	1162.9	799.9	31.21%	1800.0	965.3	919.4	4.75%	1800.0	950.4	920.7	3.13%
Avg-B	1800.0			15.46%	1800.0			3.20%	1800.0			2.25%

¹ The rows labeled Avg-A and Avg-B represent the average metric values calculated across all instances of type A and type B, respectively.

Table 6: Average computational performance of FFF across all instances using various fragment sets for DARP-LPT within a 30-minute timeframe

		S_{RF}				S_{FF}				S_{MF}			
Type	F	Net	Time	Gap	F	Net	Time	Gap	F	Net	Time	Gap	
Basic, $L = 4$	A	475.7	0.4	1542.9	2.17%	567.3	1.4	1542.9	2.03%	452.0	1.7	1543.0	1.92%
	B	579.6	0.4	1800.0	2.42%	808.0	1.5	1800.0	2.25%	506.0	1.9	1800.0	2.32%
Basic, $L = 6$	A	475.7	0.4	1107.8	0.86%	937.3	5.8	1034.5	0.68%	454.6	5.8	1057.9	0.65%
	B	579.6	0.4	1444.6	0.57%	2449.2	10.2	1422.5	0.47%	511.8	11.1	1443.4	0.45%
Extended, $L = 4$	A	661.0	0.5	1542.9	2.44%	875.3	2.2	1542.9	2.15%	612.7	3.0	1543.0	2.17%
	B	1914.0	1.7	1800.0	3.67%	3070.0	8.7	1800.0	2.87%	1376.0	8.5	1800.0	2.94%
Extended, $L = 6$	A	661.0	0.5	1031.5	0.99%	1807.3	15.0	1031.7	0.91%	620.6	14.6	1030.8	0.94%
	B	1914.0	1.9	1228.9	1.08%	20382.6	204.3	1104.4	1.25%	1495.6	202.8	1191.7	0.96%

¹ Type: instance type; F: fragment count; Net: network time, the time required for fragment generation and fragment-based network construction; Time (s) represents the total time, including preprocessing time, network time, and CPU time for solver; basic: basic instances; extended: extended instances.

Table 6 presents a comparative analysis of three fragment set types S_{RF} , S_{FF} , and

S_{MF} . These fragment sets are utilized as input for formulation FFF for solving DARP-LPT. The table covers both basic and extended instances, with $|V| = \lceil n/3 \rceil$ when $L = 4$ and $|V| = \lceil n/5 \rceil$ when $L = 6$. Due to the extensive amount of results, we present only the average metrics (fragment count, network time, total time, and gap) for all instances here. Detailed results for basic and extended instances with $L = 4$ and $L = 6$ are available in Tables 1, 2, 3, and 4 in the Appendix.

We begin by comparing the two traditional fragment sets S_{FF} and S_{RF} . The set S_{FF} is better than S_{RF} in most scenarios, particularly excelling in scenarios with a limited number of pickups per trip (e.g., $L = 4$), flexible time windows (extended instances), and increased maximum ride time (instance type B), as reflected in the columns Gap. However, for extended type B instances with $L = 6$, S_{RF} may outperform S_{FF} . This variation can be attributed to fragment count and the quality of lower bound. When L is lower, or when time windows or maximum ride time are tight, the fragment counts for S_{FF} and S_{RF} are similar or at least of the same magnitude. Conversely, when L is higher and both time windows and maximum ride time are more flexible, the fragment count for S_{FF} is substantially higher than that for S_{RF} . This is important because employing a large fragment set as input can slow down the computation process. Additionally, the fragments from S_{FF} are longer than those from S_{RF} , in a similar way as paths are longer than individual arcs. This similarity helps to explain why S_{FF} generally achieves better lower bounds than S_{RF} , because path-based (extended) formulations for routing problems typically yield superior lower bounds compared to arc-based formulations (Desrosiers et al., 2024).

The mixed fragment set S_{MF} demonstrates superior solution quality in scenarios with more flexible time windows and maximum ride time and higher values of L (extended type B instances with $L = 6$), as indicated by the gap metrics. Notably, the fragment count of S_{MF} remains relatively low, especially when compared to S_{FF} . Since a larger number of fragments can slow down fragment-based formulations, S_{MF} presents itself as an efficient alternative to S_{FF} in this regard.

5.2.2 Results for MDARP-LPT

Table 7 compares three types of fragment sets for MDARP-LPT using FFF under different parameters. Formulation FAF for DARP-LPT can be extended with additional constraints to handle also MDARP-LPT, but its performance significantly lags behind that of FFF, which is why we only present results for FFF and not FAF. The reason for not altering L is that $L = 4$ represents a commonly used parameter in carpooling scenarios (the realistic background of MDARP-LPT). Here, we present only the average metrics for

Table 7: Average computational performance of FFF across all instances using various fragment sets for MDARP-LPT within a 30-minute timeframe (basic instances with $L = 4$)

V	Type	S_{RF}				S_{FF}				S_{MF}			
		F	Net	Time	Gap	F	Net	Time	Gap	F	Net	Time	Gap
$\lceil n/4 \rceil$	A	269.1	8.2	813.9	1.50%	274.4	9.5	806.4	1.19%	162.7	69.7	777.4	0.82%
	B	1489.2	14.8	1471.1	3.02%	1650.6	20.5	1210.7	1.91%	674.4	96.6	797.5	0.78%
$\lceil n/3 \rceil$	A	201.9	10.0	636.5	0.56%	206.4	10.9	464.3	0.59%	124.3	52.7	423.5	0.31%
	B	1195.0	16.7	1107.3	1.80%	1227.6	20.0	872.0	0.55%	518.8	90.9	552.6	0.36%

¹ Type: instance type; F: fragment count; Net: network time, the time required for fragment generation and fragment-based network construction; Time (s) represents the total time, including preprocessing time, network time, and CPU time for solver.

all instances. Detailed results can be found in Table 1 and 2 in the Appendix.

Table 7 demonstrates the superiority of S_{PFF} over S_{RF} and S_{FF} in computational performance, particularly for handling large instances. This is evident from the consistently lower time and gap values achieved with S_{PFF} compared to S_{FF} . Notably, S_{PFF} 's superiority can likely be attributed to its lower fragment count. Our findings also indicate that across most instances, S_{FF} generally outperforms S_{RF} in terms of both time efficiency and solution quality.

6 Summary and conclusions

In this paper we have introduced two variants of the dial-a-ride problem, specifically MDARP-LPT and DARP-LPT. MDARP-LPT addresses scenarios where vehicles have unique origins and destinations, while DARP-LPT assumes that all vehicles begin and end their routes at a fixed depot. These problem variants are motivated by real-world carpooling and crowdshipping scenarios, where each trip can pick up at most a certain number L of customers. (M)DARP-LPT has been proven to be NP-hard through a reduction from the capacitated vehicle routing problem.

To efficiently solve both MDARP-LPT and DARP-LPT, we have applied a unified fragment-based method, where a fragment is a partial path. Our main contributions entail the extensions of a fragment-based formulation, the creation of improved fragment sets, and the insights gained from comparing fragment sets. More specifically, we have modeled (M)DARP-LPT using two fragment-based formulations, FFF and FAF, both of which are extended from the DARP fragment-based formulation of Rist & Forbes (2021), transition-

ing from fragment-based decision variables to fragment-vehicle-based variables. We find that FFF achieves better results than FAF in terms of solving time and optimality gap, which confirms our theoretical finding that FFF will also yield better lower bounds. We have also introduced improved fragment sets as formulation inputs. The two benchmark fragment sets, the full fragments set S_{FF} and the restricted fragments set S_{RF} , are generated using the methods described by Alyasiry et al. (2019) and Rist & Forbes (2021), respectively. Our two novel sets are the path-enumerated full fragment set S_{PFF} and the mixed fragment set S_{MF} . The generation of S_{PFF} involves exhaustively enumerating paths, selectively choosing those meeting specific criteria, and then decomposing them into full fragments. This approach draws inspiration from the observation that carpooling and crowdshipping DARP routes typically involve a limited number of customers. We construct the set S_{MF} by decomposing some of the full fragments in S_{FF} into restricted fragments while preserving the remainder. This approach is designed for scenarios when L is higher. All these fragment sets can be employed as input for fragment-based formulations to reach optimality. Our computational results demonstrate that for MDARP-LPT with $L = 4$, a realistic carpooling setting, S_{PFF} outperforms S_{FF} , and S_{FF} performs better than S_{RF} in terms of computational performance. For DARP-LPT, S_{FF} generally outperforms S_{RF} except when the instances have more flexible time windows, increased maximum ride times, and higher L values. In such cases, S_{MF} can replace S_{FF} to achieve the best performance.

We conclude with two supplementary observations. First, in DARP-LPT, FAF may outperform FFF for a number of small instances, as shown in Table 5. This advantage becomes more prevalent when a fixed number of vehicles is utilized. The underlying reason for this, intuitively, is that FAF, having fewer variables than FFF, solves its linear relaxations more quickly, but produces worse lower bounds. Thus, in small instances with fairly simple branch-and-bound trees, FAF tends to perform better. Conversely, in large instances, FAF’s performance tends to be worse than FFF. Additionally, when the number of vehicles is fixed, the complexity of the problem is reduced, allowing FAF to perform better than FFF in more scenarios. Second, the technique of variable fixing could be a viable option to reduce the number of fragments by removing those whose reduced cost is higher than the gap between a feasible solution’s objective value and the linear relaxation bound (Desaulniers et al., 2020). In the instances that we have tested, however, even if we set the objective value as the optimal value, this method typically removes only a small number of fragments, which hardly affects the final computational results.

References

- Achuthan, N. R., Caccetta, L., & Hill, S. P. (2003). An Improved Branch-and-Cut Algorithm for the Capacitated Vehicle Routing Problem. *Transportation Science*, *37*, 153–169. doi:10.1287/trsc.37.2.153.15243.
- Alyasiry, A. M., Forbes, M., & Bulmer, M. (2019). An exact algorithm for the pickup and delivery problem with time windows and last-in-first-out loading. *Transportation Science*, *53*, 1695–1705. doi:10.1287/trsc.2019.0905.
- Arslan, A. M., Agatz, N., Kroon, L., & Zuidwijk, R. (2019). Crowdsourced delivery—a dynamic pickup and delivery problem with ad hoc drivers. *Transportation Science*, *53*, 222–235. doi:10.1287/trsc.2017.0803.
- Baldacci, R., Bartolini, E., & Mingozzi, A. (2011). An Exact Algorithm for the Pickup and Delivery Problem with Time Windows. *Operations Research*, *59*, 414–426. doi:10.1287/opre.1100.0881.
- Bektaş, T., Gouveia, L., & Santos, D. (2020). Compact formulations for multi-depot routing problems: Theoretical and computational comparisons. *Computers and Operations Research*, *124*, 105084. doi:10.1016/j.cor.2020.105084.
- Chen, Y. (2023). Approximation schemes for capacity vehicle routing problems: A survey (working paper). URL: <https://arxiv.org/abs/2306.01826>.
- Cordeau, J.-F. (2006). A Branch-and-Cut Algorithm for the Dial-a-Ride Problem. *Operations Research*, *54*, 573–586. doi:10.1287/opre.1060.0283.
- Cornuejols, G., & Harche, F. (1993). Polyhedral study of the capacitated vehicle routing problem. *Mathematical Programming*, *60*, 21–52. doi:10.1007/BF01580599.
- Desaulniers, G., Gschwind, T., & Irnich, S. (2020). Variable Fixing for Two-Arc Sequences in Branch-Price-and-Cut Algorithms on Path-Based Models. *Transportation Science*, *54*, 1170–1188. doi:10.1287/trsc.2020.0988.
- Desrosiers, J., Lübbecke, M., Desaulniers, G., & Gauthier, J. B. (2024). *Branch-and-Price*. Technical report, Les Cahiers du GERAD G-2024-36, GERAD, HEC Montréal, Canada. URL: <https://www.gerad.ca/en/papers/G-2024-36>.

- Dessouky, M., & Mahtab, Z. (2022). *The Ridesharing Routing Problem with Flexible Pick-up and Drop-off Points*. Technical Report National Center for Sustainable Transportation, UC Davis. URL: <https://escholarship.org/uc/item/3107w642>.
- Fessler, A., Thorhauge, M., Mabit, S., & Haustein, S. (2022). A public transport-based crowdshipping concept as a sustainable last-mile solution: Assessing user preferences with a stated choice experiment. *Transportation Research Part A: Policy and Practice*, *158*, 210–223. doi:10.1016/j.tra.2022.02.005.
- Gschwind, T., & Irnich, S. (2015). Effective handling of dynamic time windows and its application to solving the dial-a-ride problem. *Transportation Science*, *49*, 335–354. doi:10.1287/trsc.2014.0531.
- Guo, X., Luo, K., Tang, Z. G., & Zhang, Y. (2022). The online food delivery problem on stars. *Theoretical Computer Science*, *928*, 13–26. doi:10.1016/j.tcs.2022.06.007.
- Jepsen, M., Petersen, B., Spoorendonk, S., & Pisinger, D. (2008). Subset-Row Inequalities Applied to the Vehicle-Routing Problem with Time Windows. *Operations Research*, *56*, 497–511. doi:10.1287/opre.1070.0449.
- Mourad, A., Puchinger, J., & Chu, C. (2019). A survey of models and algorithms for optimizing shared mobility. *Transportation Research Part B: Methodological*, *123*, 323–346. doi:10.1016/j.trb.2019.02.003.
- Rist, Y., & Forbes, M. A. (2021). A New Formulation for the Dial-a-Ride Problem. *Transportation Science*, *55*, 1113–1135. doi:10.1287/trsc.2021.1044.
- Ropke, S., & Cordeau, J.-F. (2009). Branch and Cut and Price for the Pickup and Delivery Problem with Time Windows. *Transportation Science*, *43*, 267–286. doi:10.1287/trsc.1090.0272.
- Ropke, S., Cordeau, J.-F., & Laporte, G. (2007). Models and branch-and-cut algorithms for pickup and delivery problems with time windows. *Networks*, *49*, 258–272. doi:<https://doi.org/10.1002/net.20177>.
- Savelsbergh, M. W. P., & Sol, M. (1995). The General Pickup and Delivery Problem. *Transportation Science*, *29*, 17–29. doi:10.1287/trsc.29.1.17.
- Simoni, M. D., Marcucci, E., Gatta, V., & Claudel, C. G. (2020). Potential last-mile impacts of crowdshipping services: a simulation-based evaluation. *Transportation*, *47*, 1933–1954. doi:10.1007/s11116-019-10028-4.

- Su, Y., Dupin, N., & Puchinger, J. (2023). A deterministic annealing local search for the electric autonomous dial-a-ride problem. *European Journal of Operational Research*, *309*, 1091–1111. doi:10.1016/j.ejor.2023.02.012.
- Tafreshian, A., Masoud, N., & Yin, Y. (2020). Frontiers in service science: Ride matching for peer-to-peer ride sharing: A review and future directions. *Service Science*, *12*, 40–60. doi:10.1287/serv.2020.0258.
- Zhang, W., Jacquillat, A., Wang, K., & Wang, S. (2023). Routing Optimization with Vehicle–Customer Coordination. *Management Science*, *69*, 6876–6897. doi:10.1287/mnsc.2023.4739.

A Arc-based formulation of MDARP-LPT

For MDARP-LPT, the full arc-based formulation (following Cordeau (2006)) is as follows:

Table 1: Sets, parameters, and decision variables of arc-based formulation for MDARP-LPT

Sets	Definition
N_v	Set of locations, $N = P_v \cup D_v \cup \{o_v, d_v\}$, where o_v and d_v are respectively origin and destination of vehicle $v \in V$
P_v, D_v	Pickup and delivery locations of vehicle $v \in V$
A_v	Set of location arcs of vehicle $v \in V$
Parameters	Definition
e_{iv}, l_{iv}	The earliest and latest time of vehicle v at location $i \in N$
Decision variables	Definition
f_{ijv}	=1, if the arc $(i, j) \in A_v$ is traversed by vehicle $v \in V$; =0, otherwise
t_{iv}	the departure time of vehicle v on location $i \in N_v$
Q_{iv}	the load of vehicle v after visiting location $i \in N_v$

$$\min \sum_{v \in V} \sum_{(i,j) \in A_v} C_{ij} f_{ijv} \quad (40)$$

$$s.t. \quad \sum_{v \in V} \sum_{j \in N_v} f_{ijv} = 1 \quad i \in P \quad (41)$$

$$\sum_{j \in N_v} f_{ijv} = \sum_{j \in N_v} f_{(i+n)jv} \quad i \in P_v, v \in V \quad (42)$$

$$\sum_{j \in N_v} f_{o_v j v} = 1 \quad v \in V \quad (43)$$

$$\sum_{j \in N_v} f_{jiv} = \sum_{j \in N_v} f_{ijv} \quad i \in P_v \cup D_v, v \in V \quad (44)$$

$$\sum_{i \in N_v} f_{id_v} = 1 \quad v \in V \quad (45)$$

$$t_{iv} + T_{ij} \leq t_{jv} + M_{ijv}(1 - f_{ijv}) \quad (i, j) \in A_v, v \in V \quad (46)$$

$$e_{iv} \leq t_{iv} \leq l_{iv} \quad i \in N_v, v \in V \quad (47)$$

$$Q_{iv} + q_i \leq Q_{jv} + W_{ij}(1 - f_{ijv}) \quad (i, j) \in A_v, v \in V \quad (48)$$

$$\max(0, q_i) \leq Q_{iv} \leq \min(Q, Q + q_i) \quad i \in N_v, v \in V \quad (49)$$

$$T_{i(n+i)} \leq t_{(n+i)v} - t_{iv} \leq R_i \quad i \in P_v, v \in V \quad (50)$$

$$t_{(2n+1)v} - t_{0v} \leq R_0 \quad v \in V \quad (51)$$

$$\sum_{(i,j) \in A_v} f_{ijv} \leq 2L + 1 \quad v \in V \quad (52)$$

$$f_{ijv} \in \{0, 1\} \quad (i, j) \in A_v, v \in V \quad (53)$$

To be concise, we outline the differences between the formulations of MDARP-LPT and DARP-LPT. Constraints (4) to (6) in DARP-LPT are modified to constraints (43) to (45) in MDARP-LPT, accommodating the network flow constraints for distinct vehicles with unique origins and destinations. Constraints (52) can be modified to $\sum_{(i,j) \in A_v} \max(q_i, 0) f_{ijv} \leq 2\lambda + 1$ if the constraint on the maximum number of pickups per trip is replaced by the constraint on the maximum quantity of items (or passengers) λ per trip, where q_i represents the customer load quantity. Importantly, the constraints on λ remain applicable within our fragment-based approach. The necessary modification involves updating constraint (21) in FFF and constraint (32) in FAF from $\sum_{f \in F} L_f x_{fv} \leq L$ to $\sum_{f \in F} \lambda_f x_{fv} \leq \lambda$, where λ_f represents the total quantity of items in fragment f .

B Full computational results for DARP-LPT

All four tables below serve as supplements to Table 6.

Table 1: Computational performance of FFF with different fragment sets for DARP-LPT within 30 minutes (Basic instances, $L = 4$)

S_{RF}								S_{FF}								S_{MF}							
Name	F	Net	MIP	Time	OBJ	LB	Gap	F	Net	MIP	Time	OBJ	LB	Gap	F	Net	MIP	Time	OBJ	LB	Gap		
a3-18	73	0.3	0.0	0.4	302.5	302.5	0.00%	64	0.1	0.0	0.2	302.5	302.5	0.00%	64	0.3	0.2	1.0	302.5	302.5	0.00%		
a3-30	93	0.1	1799.9	1800.0	494.8	491.0	0.75%	89	0.1	1799.9	1800.0	494.8	491.1	0.74%	89	0.5	1798.8	1800.0	494.8	489.7	1.01%		
a3-36	121	0.1	1800.5	1800.0	574.4	560.6	2.40%	112	0.2	1797.6	1800.0	574.4	565.0	1.63%	113	0.1	1799.8	1800.0	574.4	566.7	1.35%		
a4-48	318	0.2	1798.9	1800.0	697.9	686.1	1.69%	312	0.5	1799.4	1800.0	697.9	687.4	1.50%	303	0.5	1798.8	1800.0	697.9	687.9	1.43%		
a6-60	601	0.4	1793.4	1800.0	869.0	843.2	2.97%	648	1.4	1795.5	1800.0	864.9	843.4	2.48%	579	1.8	1795.7	1800.0	864.9	844.8	2.32%		
a7-70	1036	0.8	1796.3	1800.0	986.3	958.5	2.82%	1273	2.6	1792.3	1800.0	986.6	956.5	3.05%	932	2.9	1795.1	1800.0	984.9	956.5	2.88%		
a8-80	1088	0.8	1789.1	1800.0	1064.6	1016.4	4.53%	1473	5.1	1785.7	1800.0	1071.1	1019.3	4.84%	1084	6.2	1782.4	1800.0	1063.4	1016.3	4.43%		
Avg-A	475.7	0.4		1542.9			2.17%	567.3	1.4		1542.9			2.03%	452.0	1.7		1543.0			1.92%		
b3-36	169	0.1	1799.9	1800.0	576.5	566.2	1.79%	161	0.1	1799.7	1800.0	576.5	567.7	1.53%	146	0.1	1799.8	1800.0	576.5	566.1	1.81%		
b4-40	311	0.2	1799.5	1800.0	635.2	630.4	0.76%	203	0.4	1799.1	1800.0	635.2	631.1	0.64%	202	0.4	1799.5	1800.0	635.2	631.8	0.54%		
b5-50	518	0.4	1798.6	1800.0	789.1	766.2	2.91%	803	1.2	1797.6	1800.0	789.1	768.3	2.63%	496	2.2	1796.2	1800.0	789.5	766.7	2.90%		
b6-60	940	0.6	1793.3	1800.0	931.4	895.5	3.86%	1218	2.6	1792.3	1800.0	931.7	900.7	3.33%	799	2.0	1794.2	1800.0	931.7	900.4	3.36%		
b7-70	960	0.7	1796.4	1800.0	948.0	921.6	2.79%	1655	3.2	1789.5	1800.0	950.4	920.7	3.13%	887	4.6	1789.1	1800.0	950.2	921.7	3.00%		
Avg-B	579.6	0.4		1800.0			2.42%	808.0	1.5		1800.0			2.25%	506.0	1.9		1800.0			2.32%		

¹ F: fragment count; Net: network time, the time required for fragment generation and fragment-based network construction; MIP: CPU time for solver; Time (s) represents the total time, including preprocessing time, network time, and CPU time for solver. The rows labeled Avg-A and Avg-B represent the average metric values calculated across all instances of type A and type B, respectively.

Table 2: Computational performance of FFF with different fragment sets for DARP-LPT within 30 minutes (Basic instances, $L = 6$)

S_{RF}								S_{FF}								S_{MF}							
Name	F	Net	MIP	Time	OBJ	LB	Gap	F	Net	MIP	Time	OBJ	LB	Gap	F	Net	MIP	Time	OBJ	LB	Gap		
a3-18	73	0.2	0.3	1.0	295.8	295.8	0.00%	64	0.1	0.0	0.2	295.8	295.8	0.00%	64	0.1	0.0	0.2	295.8	295.8	0.00%		
a3-30	93	0.3	17.5	18.9	477.0	477.0	0.00%	89	0.1	4.5	4.7	477.0	477.0	0.00%	89	0.2	4.4	4.7	477.0	477.0	0.00%		
a3-36	121	0.1	534.4	535.0	549.8	549.8	0.00%	115	0.2	36.0	36.4	549.8	549.8	0.00%	120	0.2	200.2	200.6	549.8	549.8	0.00%		
a4-48	318	0.3	1798.6	1800.0	669.4	662.9	0.97%	342	0.7	1798.9	1800.0	669.4	664.4	0.74%	305	0.7	1798.3	1800.0	669.4	665.5	0.58%		
a6-60	601	0.4	1798.0	1800.0	825.0	819.0	0.72%	817	4.5	1796.3	1800.0	825.0	820.3	0.57%	589	3.6	1794.6	1800.0	825.0	820.6	0.54%		
a7-70	1036	0.7	1793.6	1800.0	926.7	912.4	1.54%	2114	10.8	1786.0	1800.0	927.6	912.8	1.60%	944	10.7	1786.6	1800.0	927.6	913.1	1.56%		
a8-80	1088	0.7	1790.5	1800.0	1000.9	973.1	2.77%	3020	24.2	1770.1	1800.0	991.3	973.1	1.83%	1071	25.3	1767.5	1800.0	992.8	974.0	1.89%		
Avg-A	475.7	0.4		1107.8			0.86%	937.3	5.8		1034.5			0.68%	454.6	5.8		1057.9			0.65%		
b3-36	169	0.1	22.7	23.1	557.9	557.9	0.00%	210	0.3	13.5	14.0	557.9	557.9	0.00%	154	0.3	16.2	16.8	557.9	557.9	0.00%		
b4-40	311	0.2	1799.3	1800.0	627.4	623.9	0.56%	228	1.5	1696.5	1698.5	627.4	627.4	0.00%	216	1.7	1797.9	1800.0	627.4	626.2	0.20%		
b5-50	518	0.3	1798.7	1800.0	751.9	745.3	0.87%	1868	5.9	1791.6	1800.0	751.9	744.2	1.03%	492	7.1	1793.4	1800.0	751.9	745.7	0.82%		
b6-60	940	0.6	1795.9	1800.0	877.0	868.0	1.03%	3769	14.7	1782.2	1800.0	877.0	867.1	1.13%	806	14.7	1783.4	1800.0	877.0	867.8	1.05%		
b7-70	960	0.7	1798.2	1800.0	896.4	892.9	0.39%	6171	28.5	1766.2	1800.0	896.4	894.6	0.21%	891	31.7	1765.5	1800.0	896.4	894.8	0.19%		
Avg-B	579.6	0.4		1444.6			0.57%	2449.2	10.2		1422.5			0.47%	511.8	11.1		1443.4			0.45%		

¹ F: fragment count; Net: network time, the time required for fragment generation and fragment-based network construction; MIP: CPU time for solver; Time (s) represents the total time, including preprocessing time, network time, and CPU time for solver. The rows labeled Avg-A and Avg-B represent the average metric values calculated across all instances of type A and type B, respectively.

Table 3: Computational performance of FFF with different fragment sets for DARP-LPT within 30 minutes (Extended instances, $L = 4$)

Name	S_{RF}							S_{FF}							S_{MF}						
	F	Net	MIP	Time	OBJ	LB	Gap	F	Net	MIP	Time	OBJ	LB	Gap	F	Net	MIP	Time	OBJ	LB	Gap
a3-18	96	0.1	0.3	0.4	288.5	288.5	0.00%	81	0.1	0.5	0.6	288.5	288.5	0.00%	81	0.1	0.5	0.7	288.5	288.5	0.00%
a3-30	106	0.1	1799.8	1800.0	491.4	486.6	0.97%	101	0.1	1799.7	1800.0	491.4	485.9	1.12%	101	0.1	1799.7	1800.0	491.4	486.7	0.96%
a3-36	161	0.1	1799.5	1800.0	541.9	532.2	1.79%	159	0.2	1798.7	1800.0	541.9	535.4	1.20%	155	0.2	1799.7	1800.0	541.9	536.4	1.01%
a4-48	420	0.2	1798.2	1800.0	697.8	680.2	2.52%	431	0.6	1798.0	1800.0	697.8	680.9	2.42%	407	0.7	1798.6	1800.0	697.9	679.9	2.58%
a6-60	859	0.6	1793.8	1800.0	846.1	828.9	2.04%	1026	2.3	1794.7	1800.0	847.5	830.6	1.99%	830	2.2	1793.9	1800.0	846.1	826.6	2.31%
a7-70	1502	1.2	1792.9	1800.0	971.5	939.8	3.26%	2055	5.0	1789.1	1800.0	968.3	941.4	2.78%	1285	6.8	1786.7	1800.0	968.9	940.5	2.93%
a8-80	1483	1.1	1788.7	1800.0	1073.8	1004.4	6.46%	2274	7.0	1782.7	1800.0	1065.2	1006.0	5.56%	1430	10.7	1771.7	1800.0	1060.3	1003.0	5.41%
Avg-A	661.0	0.5		1542.9			2.44%	875.3	2.2		1542.9			2.15%	612.7	3.0		1543.0			2.17%
b3-36	460	0.3	1799.4	1800.0	556.5	540.9	2.80%	567	0.6	1799.1	1800.0	556.5	542.9	2.45%	435	0.7	1797.7	1800.0	556.5	544.0	2.25%
b4-40	910	0.6	1798.1	1800.0	582.8	571.0	2.02%	906	2.1	1797.4	1800.0	582.8	573.4	1.61%	614	1.8	1797.2	1800.0	582.8	573.8	1.55%
b5-50	1686	1.4	1792.0	1800.0	755.1	730.2	3.30%	3196	12.4	1785.3	1800.0	754.7	732.3	2.97%	1348	7.7	1789.4	1800.0	754.7	731.5	3.07%
b6-60	3036	2.9	1790.3	1800.0	873.8	837.0	4.21%	3890	9.6	1781.1	1800.0	868.9	841.7	3.13%	1929	10.5	1782.0	1800.0	874.6	842.0	3.73%
b7-70	3478	3.4	1753.1	1800.0	911.6	856.7	6.02%	6791	18.8	1762.9	1800.0	900.4	862.7	4.19%	2554	21.8	1755.4	1800.0	897.1	860.5	4.09%
Avg-B	1914.0	1.7		1800.0			3.67%	3070.0	8.7		1800.0			2.87%	1376.0	8.5		1800.0			2.94%

¹ F: fragment count; Net: network time, the time required for fragment generation and fragment-based network construction; MIP: CPU time for solver; Time (s) represents the total time, including preprocessing time, network time, and CPU time for solver. The rows labeled Avg-A and Avg-B represent the average metric values calculated across all instances of type A and type B, respectively.

Table 4: Computational performance of FFF with different fragment sets for DARP-LPT within 30 minutes (Extended instances, $L = 6$)

Name	S_{RF}							S_{FF}							S_{MF}						
	F	Net	MIP	Time	OBJ	LB	Gap	F	Net	MIP	Time	OBJ	LB	Gap	F	Net	MIP	Time	OBJ	LB	Gap
a3-18	96	0.0	0.9	1.0	282.4	282.4	0.00%	88	0.1	0.6	0.8	282.4	282.4	0.00%	90	0.3	1.9	2.5	282.4	282.4	0.00%
a3-30	106	0.1	11.9	12.2	472.5	472.5	0.00%	101	0.1	9.4	9.7	472.5	472.5	0.00%	101	0.3	8.2	8.7	472.5	472.5	0.00%
a3-36	161	0.1	6.9	7.5	510.6	510.6	0.00%	179	0.4	10.6	11.6	510.6	510.6	0.00%	158	0.3	3.6	4.2	510.6	510.6	0.00%
a4-48	420	0.3	1798.6	1800.0	661.2	656.5	0.70%	501	1.3	1797.6	1800.0	661.2	657.7	0.52%	404	1.3	1797.6	1800.0	661.2	657.4	0.57%
a6-60	859	0.6	1797.8	1800.0	807.1	796.7	1.29%	1623	9.6	1790.0	1800.0	807.1	797.7	1.17%	833	9.8	1788.7	1800.0	807.1	797.6	1.18%
a7-70	1502	1.1	1794.6	1800.0	908.5	891.3	1.89%	4266	26.8	1766.3	1800.0	907.9	891.7	1.79%	1341	28.1	1767.3	1800.0	908.5	892.6	1.75%
a8-80	1483	1.1	1782.0	1800.0	988.3	958.3	3.03%	5893	66.6	1720.0	1800.0	986.9	958.2	2.90%	1417	62.1	1727.7	1800.0	989.3	959.1	3.06%
Avg-A	661.0	0.5		1031.5			0.99%	1807.3	15.0		1031.7			0.91%	620.6	14.6		1030.8			0.94%
b3-36	460	0.2	9.0	9.7	530.6	530.6	0.00%	1199	2.5	18.6	22.1	530.6	530.6	0.00%	436	2.2	12.0	14.9	530.6	530.6	0.00%
b4-40	910	0.7	733.4	734.9	564.6	564.6	0.00%	2247	18.0	80.7	99.9	564.6	564.6	0.00%	676	18.5	524.5	543.8	564.6	564.6	0.00%
b5-50	1686	1.4	1795.4	1800.0	710.8	701.4	1.33%	17112	90.7	1699.1	1800.0	710.8	703.0	1.10%	1420	94.8	1701.4	1800.0	710.8	702.8	1.14%
b6-60	3036	3.1	1793.6	1800.0	817.8	799.3	2.26%	22909	177.8	1600.9	1800.0	818.7	799.3	2.38%	2135	185.2	1609.2	1800.0	818.3	804.5	1.69%
b7-70	3478	4.1	1778.4	1800.0	837.7	822.7	1.79%	58446	732.6	957.9	1800.0	844.8	821.3	2.78%	2811	713.3	1075.2	1800.0	841.0	824.5	1.97%
Avg-B	1914.0	1.9		1228.9			1.08%	20382.6	204.3		1104.4			1.25%	1495.6	202.8		1191.7			0.96%

¹ F: fragment count; Net: network time, the time required for fragment generation and fragment-based network construction; MIP: CPU time for solver; Time (s) represents the total time, including preprocessing time, network time, and CPU time for solver. The rows labeled Avg-A and Avg-B represent the average metric values calculated across all instances of type A and type B, respectively.

C Full computational results for MDARP-LPT

Both tables below serve as supplements to Table 7. One point worth noting is that while the instances used in both tables are derived from Cordeau, they are not identical since we modify the number of vehicles and the number of customers (see Table 4 for details).

Table 1: Computational performance of FFF with different fragment sets for MDARP-LPT within 30 minutes (basic instances: $|V| = \lceil n/4 \rceil$, $L = 4$)

	S_{RF}							S_{FF}							S_{FFF}						
	F	Net	MIP	Time	OBJ	LB	Gap	F	Net	MIP	Time	OBJ	LB	Gap	F	Net	MIP	Time	OBJ	LB	Gap
a3-18	45	8.9	0.5	9.4	239.6	239.6	0.00%	40	6.2	0.4	6.6	239.6	239.6	0.00%	35	17.9	0.7	18.7	239.6	239.6	0.00%
a3-30	42	7.9	1.4	9.4	357.9	357.9	0.00%	42	9.6	2.1	11.9	357.9	357.9	0.00%	40	10.2	1.2	11.4	357.9	357.9	0.00%
a3-36	51	6.5	47.1	53.7	474.8	474.8	0.00%	48	8.0	31.3	39.5	474.8	474.8	0.00%	37	11.1	38.1	49.2	474.8	474.8	0.00%
a4-48	182	6.8	217.5	224.7	499.1	499.1	0.00%	166	6.9	179.6	186.8	499.1	499.1	0.00%	124	21.0	131.0	152.2	499.1	499.1	0.00%
a6-60	236	7.2	1791.4	1800.0	632.1	624.9	1.14%	210	8.3	1791.2	1800.0	632.1	625.7	1.00%	150	52.3	1557.4	1610.2	632.1	632.1	0.00%
a7-70	715	10.3	1788.5	1800.0	646.9	619.6	4.23%	687	13.0	1786.1	1800.0	644.6	622.7	3.40%	364	183.5	1615.6	1800.0	639.9	625.9	2.19%
a8-80	613	10.1	1788.7	1800.0	753.6	714.7	5.16%	728	14.2	1784.6	1800.0	747.4	718.0	3.93%	389	192.2	1606.8	1800.0	746.7	720.1	3.56%
Avg-A	269.1	8.2		813.9			1.50%	274.4	9.5		806.4			1.19%	162.7	69.7		777.4			0.82%
b3-36	203	6.6	148.7	155.5	425.6	425.6	0.00%	227	8.3	479.7	488.2	425.6	425.6	0.00%	133	12.7	181.1	193.8	425.6	425.6	0.00%
b4-40	518	9.7	1789.8	1800.0	405.9	402.4	0.85%	502	8.8	156.0	165.1	405.9	405.9	0.00%	260	24.2	132.4	156.8	405.9	405.9	0.00%
b5-50	1878	20.9	1777.6	1800.0	497.5	480.1	3.51%	1903	15.6	1783.3	1800.0	494.3	488.4	1.20%	865	44.8	432.3	477.6	494.3	494.3	0.00%
b6-60	2537	17.4	1779.9	1800.0	603.1	574.4	4.77%	2334	23.5	1774.6	1800.0	597.8	589.9	1.33%	969	127.6	1230.6	1359.3	596.6	596.5	0.00%
b7-70	2310	19.5	1777.3	1800.0	610.8	574.4	5.96%	3287	46.4	1750.2	1800.0	625.7	581.8	7.02%	1145	273.7	1525.2	1800.0	609.0	585.3	3.89%
Avg-B	1489.2	14.8		1471.1			3.02%	1650.6	20.5		1210.7			1.91%	674.4	96.6		797.5			0.78%

¹ F: fragment count; Net: network time, the time required for fragment generation and fragment-based network construction; MIP: CPU time for solver; Time (s) represents the total time, including preprocessing time, network time, and CPU time for solver. The rows labeled Avg-A and Avg-B represent the average metric values calculated across all instances of type A and type B, respectively.

Table 2: Computational performance of FFF with different fragment sets for MDARP-LPT within 30 minutes (basic instances: $|V| = \lceil n/3 \rceil$, $L = 4$)

	S_{RF}							S_{FF}							S_{PFF}						
	F	Net	MIP	Time	OBJ	LB	Gap	F	Net	MIP	Time	OBJ	LB	Gap	F	Net	MIP	Time	OBJ	LB	Gap
a3-18	37	7.5	0.7	8.2	229.2	229.2	0.00%	33	15.1	1.3	16.5	229.2	229.2	0.00%	29	8.0	0.3	8.4	229.2	229.2	0.00%
a3-30	36	6.9	0.6	7.6	325.8	325.8	0.00%	36	7.5	0.6	8.2	325.8	325.8	0.00%	34	7.0	2.0	9.2	325.8	325.8	0.00%
a3-36	47	9.1	5.9	15.1	397.2	397.2	0.00%	44	6.3	6.5	12.9	397.2	397.2	0.00%	34	15.2	4.0	19.3	397.2	397.2	0.00%
a4-48	116	8.3	40.0	48.6	450.8	450.8	0.01%	109	10.0	27.5	37.9	450.8	450.8	0.00%	92	21.1	23.7	45.1	450.8	450.8	0.00%
a6-60	175	9.3	766.0	775.9	556.1	556.1	0.00%	155	7.5	490.1	498.0	556.1	556.1	0.00%	113	40.3	396.6	437.4	556.1	556.1	0.00%
a7-70	507	12.0	1786.8	1800.0	552.5	549.8	0.48%	482	14.2	861.7	876.9	552.5	552.5	0.00%	250	139.2	504.8	645.1	552.5	552.5	0.00%
a8-80	495	16.9	1781.1	1800.0	663.9	641.2	3.41%	586	15.9	1783.0	1800.0	670.7	642.9	4.15%	318	137.9	1661.4	1800.0	661.8	647.6	2.14%
Aver-A	201.9	10.0		636.5			0.56%	206.4	10.9		464.3			0.59%	124.3	52.7		423.5			0.31%
b3-36	146	8.3	72.9	81.9	389.3	389.3	0.00%	148	9.5	36.9	46.9	389.3	389.3	0.00%	100	15.2	27.6	42.9	389.3	389.3	0.00%
b4-40	370	8.7	45.6	54.7	355.7	355.7	0.00%	314	8.6	23.5	32.3	355.7	355.7	0.00%	178	21.0	16.3	37.5	355.7	355.7	0.00%
b5-50	1649	16.8	1781.2	1800.0	436.3	427.0	2.12%	1635	20.4	659.2	680.9	436.3	436.3	0.00%	753	45.4	298.9	344.9	436.3	436.3	0.00%
b6-60	2269	31.3	1763.9	1800.0	527.9	512.3	2.95%	2041	28.8	1768.7	1800.0	527.7	522.6	0.98%	816	139.1	397.4	537.9	527.7	527.7	0.00%
b7-70	1541	18.6	1778.4	1800.0	530.5	509.6	3.93%	2000	32.5	1764.2	1800.0	528.4	519.1	1.76%	747	233.9	1565.0	1800.0	528.4	518.8	1.81%
Aver-B	1195.0	16.7		1107.3			1.80%	1227.6	20.0		872.0			0.55%	518.8	90.9		552.6			0.36%

¹ F: fragment count; Net: network time, the time required for fragment generation and fragment-based network construction; MIP: CPU time for solver; Time (s) represents the total time, including preprocessing time, network time, and CPU time for solver. The rows labeled Avg-A and Avg-B represent the average metric values calculated across all instances of type A and type B, respectively.